Single-Photon Detection by a Dirty Current-Carrying Superconducting Strip Based on the Kinetic-Equation Approach

D. Yu. Vodolazov

Institute for Physics of Microstructures, Russian Academy of Sciences,
603950 Nizhny Novgorod, GSP-105, Russia

Using a kinetic-equation approach, we study the dynamics of electrons and phonons in current-carrying superconducting nanostrips after the absorption of a single photon of the near-infrared or optical range. We find that the larger the $C_e/C_{\rm ph}|_{T_c}$ ratio (where T_c is the critical temperature of a superconductor and C_e and $C_{\rm ph}$ are specific heat capacities of electrons and phonons, respectively), the larger the portion of the photon's energy goes to electrons. The electrons become more strongly heated and hence can thermalize faster during the initial stage of hot-spot formation. The thermalization time $\tau_{\rm th}$ can be less than 1 ps for superconductors with $C_e/C_{\rm ph}|_{T_c} \gg 1$ and a small diffusion coefficient of $D \simeq 0.5 \ {\rm cm^2/s}$ when thermalization occurs, mainly due to electron-phonon and phonon-electron scattering in a relatively small volume of approximately $\xi^2 d$ (ξ is a superconducting coherence length, while $d < \xi$ is a thickness of the strip). For longer time spans, due to diffusion of hot electrons' effective temperature inside the hot spot decreases, the size of the hot spot increases, the superconducting state becomes unstable, and the normal domain spreads in the strip at a current larger than the so-called detection current. We find the dependence of the detection current on the photon's energy, the location of its absorption in the strip, the width of the strip, and the magnetic field, and we compare this dependence with existing experiments. Our results demonstrate that materials with $C_e/C_{\rm ph}|_{T_c} \ll 1$ are bad candidates for single-photon detectors due to a small transfer of the photon's energy to electronic system and a large $\tau_{\rm th}$. We also predict that even a several-micron-wide dirty superconducting bridge is able to detect a single near-infrared or optical photon if its critical current exceeds 70% of the depairing current and $C_e/C_{\rm ph}|_{T_c} \gtrsim 1$.

I. INTRODUCTION

The main idea of single-photon detection by the current-carrying superconducting strip is relatively simple. The absorbed photon heats the electrons in the restricted area of the strip (which is called a hot spot), superconductivity is locally destroyed, and the critical current I_c of the strip is reduced up to $I_c^{\rm spot} < I_c$. If the transport current exceeds $I_c^{\rm spot}$, a transition to the resistive state occurs, and it is detected in an experiment.

At the present time, there are several phenomenological models which offer different scenarios for the appearance of a resistive response after photon absorption and which explain certain experimental results [1–6] (see also a recent review of such models in Ref. [7]). The drawback of these models is that they use phenomenological assumptions about the size of the hot region, the level of suppression of the superconductivity, and the part of the photon's energy which is stored in the electronic system. Besides, some of these models [1,4,6] operate with the number of nonequilibrium quasiparticles in order to find the suppression of the magnitude of the superconducting order parameter $|\Delta|$. One should keep in mind that this approach is quantitatively

valid only when the deviation of the quasiparticle (electron) distribution function n from equilibrium occurs in the narrow energy interval $\delta\epsilon$ near the superconducting gap $\epsilon_g \gg \delta\epsilon$, which is not true in the case of the hot-spot formation in a thin superconducting strip—especially at its initial stage, when the effective temperature of electrons can be several times larger than the bath temperature. Therefore, one can expect only qualitative validity of the approaches using ideas of the Rothwarf-Taylor model [8].

Below, we formulate two problems which we solve to understand what material could be a good candidate for usage in a superconducting nanowire single-photon detector. The first problem concerns the question regarding which part of the energy of the photon goes to the electronic system and how it is related to material parameters of the superconducting strip. The second problem is connected with the question of how fast the electrons (throughout the paper, by electrons we mean quasiparticle excitations) are thermalized and what the role of electron-electron inelastic scattering is. It is known that all materials which show a good ability to detect single photons are extremely dirty superconducting strips with a small diffusion coefficient of $D \simeq 0.5 \ {\rm cm^2/s}$ and a

low critical temperature of $T_c \lesssim 10$ K. First, a small D does not allow fast diffusion of electrons, which favors their fast thermalization because the energy of absorbed photon is confined to a relatively small volume at the initial stage of hot-spot formation, leading to a relatively high "temperature" of the hot electrons. Second, the smaller D is, the smaller the electron-electron inelastic relaxation time $\tau_{e\text{-}e}$, which also decreases the thermalization time τ_{th} and increases the capability to detect a single photon. Indeed, if the thermalization time τ_{th} of the electrons is larger than their diffusion time $\tau_{D,w} \simeq w^2/4D$ across the strip, with width w, the photon's energy will be smeared over a large area, which leads to a smaller influence on superconducting properties and complicates the photon's detection.

To answer the above questions, we numerically solve kinetic equations for electron and phonon distribution functions, taking into account electron-phonon, phonon-electron, and electron-electron scattering. First, we study the initial stage of the electron-phonon down-conversion cascade on a time scale comparable to the characteristic time of the variation of $|\Delta|$—$\tau_\Delta \simeq \hbar/|\Delta| \simeq \hbar/k_B T_c$—during which one cannot expect a strong suppression of the superconducting order parameter and where electrons diffuse at a distance of only approximately $\sqrt{D\tau_{|\Delta|}}$, which is of about the superconducting coherence length in dirty superconductors $\xi \sim \sqrt{\hbar D/|\Delta|}$. We find that electron-phonon down-conversion cascade and thermalization in an electronic system depends not only on the strength of the electron-electron scattering but also on the ratio of electronic C_e and phonon C_{ph} heat capacities taken at $T = T_c$. Indeed, the larger the ratio $C_e/C_{ph}|_{T_c}$ is, the larger the portion of the photon's energy that goes to the electronic system. Its effective temperature becomes higher and the thermalization time τ_{th} shorter. We show that a relatively short $\tau_{th} \simeq \tau_{|\Delta|}$ can be reached in superconductors with a large $C_e/C_{ph}|_{T_c} \gg 1$ ratio when thermalization occurs, mainly via electron-phonon and phonon-electron scattering.

We study the dynamics of a hot spot at times $t \gtrsim \tau_{|\Delta|}$ for two limits. For the limit with a short thermalization time ($\tau_{th} \simeq \tau_{|\Delta|} \ll \tau_{D,w}$), we use a two-temperature model and solve heat-conduction equations (taking into account the Joule dissipation) for electron and phonon temperatures coupled with a modified Ginzburg-Landau equation for the superconducting order parameter. For the limit with a large thermalization time ($\tau_{th} \simeq \tau_{D,w}$), we assume a uniform distribution of electron and phonon effective temperatures across the strip by the time $t \simeq \tau_{D,w}$. For both limits, we find the current-energy relation and the dependence of the cutoff photon's energy on the temperature at a fixed ratio $I/I_{dep}(T)$ (I_{dep} is a depairing current),

and we study the role of the magnetic field and how the current-energy relation depends on the strip's width. We show that a relatively narrow (width of about 100–200 nm) superconducting strip with a small ratio of $C_e/C_{ph}|_{T_c} \ll 1$ needs a current close to I_{dep} to be able to detect a single photon with energy of about 1 eV. On the contrary, such a strip with a ratio of $C_e/C_{ph}|_{T_c} \gtrsim 1$ can detect the same photon at a current much smaller than the depairing current. Finally, we predict that even wide a superconducting strip with $C_e/C_{ph}|_{T_c} \gtrsim 1$ and a width of about several microns can detect a single infrared or optical photon if the strip can be biased, without a loss of superconductivity, at $I \gtrsim 0.7 I_{dep}(T)$.

The structure of the paper is as follows. In Sec. II, we present the basic equations. In Sec. III, we show results for the initial stage of hot-spot formation (on a time scale of about $\tau_{|\Delta|}$ after the photon's absorption), when its radius is smaller than the coherence length. In Sec. IV, we study the case where instability of the superconducting state occurs at the moment where the hot electrons reach both edges of the strip and form a hot belt (the limit of a large τ_{th}), while, in Sec. V, we consider the opposite case, where the superconducting state becomes unstable before the hot spot expands across the strip (the limit of a small τ_{th}). In Sec. VI, we compare our results with existing theories and experiments. In Sec. VII, we deliver our main results.

II. EQUATIONS

In this section, we present equations which we use to study the dynamics of electron and phonon distribution functions in a superconducting strip at the initial stage of hot-spot formation after absorption of the single photon. First, here are the kinetic equations for energy, time- and coordinate-dependent electron n, and phonon-N distribution functions:

$$N_1 \frac{\partial n}{\partial t} = D\nabla[(N_1^2 - R_2^2)\nabla n] - R_2 \frac{\partial n}{\partial \epsilon} \frac{\partial |\Delta|}{\partial t}$$
$$+ I_{e\text{-}ph}(n, N) + I_{e\text{-}e}(n), \tag{1}$$

$$\frac{\partial N}{\partial t} = -\frac{N - N^{eq}}{\tau_{esc}} + I_{ph\text{-}e}(N, n), \tag{2}$$

where N_1 and R_2 are spectral functions [for their definitions, see the text below Eq. (9)], $N^{eq} = 1/[\exp(\epsilon/k_B T) - 1]$ is an equilibrium distribution function of the phonons, and $I_{e\text{-}ph}(n, N)$, $I_{ph\text{-}e}(N, n)$, and $I_{e\text{-}e}(n)$ are the electron-phonon, phonon-electron, and electron-electron collision integrals:

$$I_{e\text{-ph}}(n,N) = -\frac{1}{(k_B T_c)^3}\frac{1}{\tau_0}\left[\int_0^\epsilon d\epsilon_1 M(\epsilon,\epsilon_1)(\epsilon-\epsilon_1)^2[[1+2N_{\epsilon-\epsilon_1}](n_\epsilon - n_{\epsilon_1}) + n_\epsilon(1-2n_{\epsilon_1}) + n_{\epsilon_1}]\right.$$

$$+ \int_\epsilon^{\epsilon+\hbar\omega_D} d\epsilon_1 M(\epsilon,\epsilon_1)(\epsilon-\epsilon_1)^2[[1+2N_{\epsilon_1-\epsilon}](n_\epsilon - n_{\epsilon_1}) - n_\epsilon(1-2n_{\epsilon_1}) - n_{\epsilon_1}]$$

$$\left.+ \int_0^{\hbar\omega_D-\epsilon} d\epsilon_1 M(\epsilon,-\epsilon_1)(\epsilon+\epsilon_1)^2[[1+2N_{\epsilon_1+\epsilon}](n_\epsilon + n_{\epsilon_1} - 1) - n_\epsilon(1-2n_{\epsilon_1}) - n_{\epsilon_1} + 1]\right], \quad (3)$$

$$I_{\text{ph-}e}(N,n) = \frac{\gamma}{\tau_0 k_B T_c}\left[\int_0^\epsilon d\epsilon_1 M[\epsilon_1, -(\epsilon-\epsilon_1)][n_{\epsilon_1}n_{\epsilon-\epsilon_1} + N_\epsilon(n_{\epsilon-\epsilon_1} + n_{\epsilon_1} - 1)]\right.$$

$$\left.+ 2\int_0^\infty d\epsilon_1 M[\epsilon_1, (\epsilon+\epsilon_1)][(1-n_{\epsilon_1})n_{\epsilon+\epsilon_1} + N_\epsilon(n_{\epsilon+\epsilon_1} - n_{\epsilon_1})]\right], \quad (4)$$

$$M(\epsilon, \pm\epsilon_1) = N_1(\epsilon)N_1(\epsilon_1) \mp R_2(\epsilon)R_2(\epsilon_1),$$

$$I_{e\text{-}e}(n) = \frac{\alpha_{e\text{-}e}}{\tau_0 k_B T_c}\int_0^\infty\int_0^\infty d\epsilon_1 d\epsilon_2\left[\frac{E_1}{|\epsilon-\epsilon_1|}[n_\epsilon(1-n_{\epsilon_1})(1-n_{\epsilon_2})(1-n_{\epsilon-\epsilon_1-\epsilon_2}) - (1-n_\epsilon)n_{\epsilon_1}n_{\epsilon_2}n_{\epsilon-\epsilon_1-\epsilon_2}]H_v(\epsilon-\epsilon_1-\epsilon_2)\right.$$

$$+ E_2\left(\frac{1}{|\epsilon+\epsilon_1|} + \frac{2}{|\epsilon-\epsilon_2|}\right)[n_\epsilon n_{\epsilon_1}(1-n_{\epsilon_2})(1-n_{\epsilon+\epsilon_1-\epsilon_2}) - (1-n_\epsilon)(1-n_{\epsilon_1})n_{\epsilon_2}n_{\epsilon+\epsilon_1-\epsilon_2}]H_v(\epsilon+\epsilon_1-\epsilon_2)$$

$$\left.+ E_3\left(\frac{1}{|\epsilon-\epsilon_1|} + \frac{2}{|\epsilon+\epsilon_2|}\right)[n_\epsilon(1-n_{\epsilon_1})n_{\epsilon_2}n_{\epsilon_1-\epsilon_2-\epsilon} - (1-n_\epsilon)n_{\epsilon_1}(1-n_{\epsilon_2})(1-n_{\epsilon_1-\epsilon_2-\epsilon})]H_v(\epsilon_1-\epsilon_2-\epsilon)\right], \quad (5)$$

$$E_1 = a[N_1(\epsilon)N_1(\epsilon_1)N_1(\epsilon_2)N_1(\epsilon-\epsilon_1-\epsilon_2)$$
$$- R_2(\epsilon)R_2(\epsilon_1)R_2(\epsilon_2)R_2(\epsilon-\epsilon_1-\epsilon_2)]$$
$$+ b[N_1(\epsilon)R_2(\epsilon_1)R_2(\epsilon_2)N_1(\epsilon-\epsilon_1-\epsilon_2)$$
$$- R_2(\epsilon)N_1(\epsilon_1)N_1(\epsilon_2)R_2(\epsilon-\epsilon_1-\epsilon_2)].$$

Coefficients E_2 and E_3 are expressed via E_1 in the following way: $E_2 = E_1(\epsilon_1 \to -\epsilon_1)$, $E_3 = E_1(\epsilon \to -\epsilon, \epsilon_1 \to -\epsilon_1)$. a and b are coefficients on the order of unity [9,10] and $H_v(x)$ is a Heaviside function.

$I_{e\text{-ph}}(n,N)$ and $I_{\text{ph-}e}(N,n)$ are written above for a case where one can neglect the renormalization of the electron-phonon coupling constant due to disorder [11,12], and

$$\frac{1}{\tau_0} = g\left(\frac{k_B T_c}{\hbar\omega_D}\right)^2\frac{k_B T_c}{\hbar} \quad (6)$$

is the familiar characteristic time introduced in Ref. [11] (ω_D is a Debye frequency and g is an electron-phonon coupling constant). Coefficient

$$\gamma = \frac{4\hbar\omega_D N(0)}{9N_{\text{ion}}}\left(\frac{\hbar\omega_D}{k_B T_c}\right)^2 = \frac{8\pi^2}{5}\left.\frac{C_e}{C_{\text{ph}}}\right|_{T=T_c}, \quad (7)$$

staying in front of the $I_{\text{ph-}e}$ collision integral, is proportional to the ratio of the electronic $C_e(T) = (2\pi^2/3)k_B^2 N(0)T$

and phonon $C_{\text{ph}}(T) = (12\pi^4/5)N_{\text{ion}}k_B(k_B T/\hbar\omega_D)^3$ specific heat capacities at $T = T_c$ [$N(0)$ is the one-spin density of states of electrons in the normal state at the Fermi energy E_F, while N_{ion} is the density of the ions].

The electron-electron collision integral in the form of Eq. (5) is written for a dirty quasi-2D metallic superconducting film with a renormalized electron-electron coupling constant due to impurities. Coefficient $\alpha_{e\text{-}e}$,

$$\alpha_{e\text{-}e} = \tau_0\frac{k_B T_c}{4\hbar}\frac{R_\square}{R_Q}, \quad (8)$$

describes the strength of electron-electron inelastic scattering ($R_\square$ is the sheet resistance and $R_Q = 2\pi\hbar/e^2 \simeq 25.8$ kΩ is the quantum resistance). In clean metal coefficients $1/|\epsilon \pm \epsilon_{1,2}|$ are absent and Eq. (5) transfers [with $\alpha_{e\text{-}e} = \tau_0(k_B T_c)^2/(2\hbar E_F)$] to an expression present in Refs. [9,10]. In the normal state, $E_1 = E_2 = E_3 = a$, and Eq. (5) coincides [with $\alpha_{e\text{-}e} = \tau_0 k_B T_c/(4\hbar k_F l)$ and $a = 1$] with an e-e collision integral for a 2D dirty metal from Ref. [13]. For dirty quasi-2D metallic normal film from Eqs. (1)–(5) and $\epsilon \gg k_B T$, the familiar inelastic e-e scattering time $\tau_{e\text{-}e}(\epsilon) = 4\hbar R_Q/(\epsilon R_\square)$ follows [see Eq. (4.4) in Ref. [14]].

Because the coefficients a and b are unknown for any metal, we put $a = 1$ and $b = 0$. The choice of $b = 0$ is

connected with different expressions for E_i behind b which are present in Refs. [9,10]. If we choose an expression for E_i from Ref. [10] (as we do in our work), a finite $b > 0$ leads to an increase of $\tau_{e\text{-}e}$ for electrons having energy close to $|\Delta|$.

The spectral functions $N_1(\epsilon)$ and $R_2(\epsilon)$ entering Eqs. (1) and (3)–(5) have to be found in the dirty limit from the Usadel equation

$$\hbar D \nabla^2 \Theta + \left(2i\epsilon - \frac{D}{\hbar}q_s^2 \cos\Theta\right)\sin\Theta + 2|\Delta|\cos\Theta = 0,$$

(9)

where $q_s = mv_s = \hbar(\nabla\phi - 2eA/\hbar c)$ is the superfluid momentum, ϕ is a phase of the superconducting order parameter $\Delta = |\Delta|e^{i\phi}$, $\cos\Theta = N_1(\epsilon) + iR_1(\epsilon)$, and $\sin\Theta = N_2(\epsilon) + iR_2(\epsilon)$. $N_1(\epsilon)N(0)$ indicates the density of states of the electrons in the superconducting state, while R_2 enters the equation for the superconducting order parameter.

A static self-consistency equation for the magnitude of the order parameter has the following form:

$$\frac{1}{\lambda_{\text{BCS}}} = \int_0^{\hbar\omega_D} \frac{R_2}{|\Delta|}(1 - 2n)d\epsilon$$
$$= \int_0^{\hbar\omega_D} \frac{R_2}{|\Delta|}(1 - 2n^{\text{eq}})d\epsilon - \Phi_{\text{neq}},$$

(10)

where $n^{\text{eq}} = 1/[\exp(\epsilon/k_B T) + 1]$ is an equilibrium distribution function of electrons (quasiparticles) and λ_{BSC} is a coupling constant in BCS theory. The suppression of $|\Delta|$ due to hot electrons is described by Φ_{neq},

$$\Phi_{\text{neq}} = 2\int_0^{\hbar\omega_D} \frac{R_2}{|\Delta|}(n - n^{\text{eq}})d\epsilon.$$

(11)

Very often, to describe the suppression of the order parameter due to $n \neq n^{\text{eq}}$, the coordinate-dependent density of the nonequilibrium electrons is used, which is determined as

$$N_{\text{neq}}(\vec{r})/V = 4N(0)\int_0^\infty N_1[n(\vec{r}) - n^{\text{eq}}]d\epsilon$$
$$= 4N(0)\int_{|\Delta|}^\infty \frac{\epsilon[n(\vec{r}) - n^{\text{eq}}]}{\sqrt{\epsilon^2 - |\Delta|^2}}d\epsilon.$$

(12)

The last expression is valid when one can neglect the gradient term and the term with q_s^2 in the Usadel equation, which leads to

$$N_1(\epsilon) = \frac{\epsilon}{\sqrt{\epsilon^2 - |\Delta|^2}}H_v(\epsilon - |\Delta|)$$

(13)

and

$$R_2(\epsilon) = \frac{|\Delta|}{\sqrt{\epsilon^2 - |\Delta|^2}}H_v(\epsilon - |\Delta|).$$

(14)

The potential Φ_{neq} can be expressed via N_{neq}/V when a deviation from equilibrium occurs in the narrow energy interval near $|\Delta|$ and one can replace $\epsilon \simeq |\Delta|$ in the numerator of Eq. (12) and take it off the integrand:

$$\Phi_{\text{neq}}(\vec{r}) = 2\int_{|\Delta|}^{\hbar\omega_D} \frac{n(\vec{r}) - n_{\text{eq}}}{\sqrt{\epsilon^2 - |\Delta|^2}}d\epsilon \simeq \frac{N_{\text{neq}}(\vec{r})}{2N(0)|\Delta|V}.$$

(15)

When the deviation from equilibrium occurs in a wide energy interval and/or it occurs at energies $\epsilon \gg |\Delta|$, then $\Phi_{\text{neq}} \neq N_{\text{neq}}/2N(0)|\Delta|V$ due to the presence of an extra factor ϵ in the numerator of Eq. (12). In this case, usage of the approach with a number of nonequilibrium electrons cannot pretend to be a quantitative description and may be used only as a qualitative analysis.

III. INITIAL STAGE OF HOT-SPOT FORMATION

When a deviation n from n^{eq} occurs in a volume smaller than ξ^3 and on a time scale shorter than a variation time of $|\Delta|$, one cannot expect a strong suppression of superconductivity. Therefore, as a first approximation, at times $t < \tau_{|\Delta|}$ we study dynamics of n and N after an absorption of the photon with $|\Delta| = \text{const}$. To further simplify the problem, we also assume that the energy of the photon is distributed instantly over the volume $V_{\text{init}} = \pi\xi^2 d$ (where $d < \xi$ is the thickness of the strip). In reality, it takes a time of about $\xi^2/D = \tau_{|\Delta|}$; we argue below that such a simplification should not change the main result of this section.

With the above assumptions, we numerically solve Eqs. (1)–(5), where we omit the gradient terms and consider the case of zero current, $I = 0$ (a finite I leads to a smearing of the spectral functions at $\epsilon \simeq |\Delta|$ and does not influence our main result). We use different initial conditions, which corresponds to different physical situations. The electronic-bubble initial condition,

$$n_\epsilon(t = 0) = n^{\text{eq}} + \frac{\alpha e^{-(\epsilon-\epsilon_0)^2/\delta\epsilon^2}}{\sqrt{\pi}\delta\epsilon},$$
$$N_\epsilon(t = 0) = N^{\text{eq}},$$

(16)

corresponds to the absorption of the photon and the creation of initial hot electron and hole quasiparticles at the energy $\epsilon \simeq \epsilon_0 \gg \delta\epsilon$.

The phonon-bubble initial condition,

$$n_\epsilon(t = 0) = n^{\text{eq}},$$
$$N_\epsilon(t = 0) = N^{\text{eq}} + \frac{\beta e^{-(\epsilon-\epsilon_0)^2/\delta\epsilon^2}}{\sqrt{\pi}\delta\epsilon},$$

(17)

models a situation where, for example, the molecule hits the strip and excites phonons with the energy $\epsilon \simeq \epsilon_0$.

Instead of a photon bubble, one can use a phonon-plateau initial condition (when acoustic phonons of all available energies $0 \leq \epsilon \leq \hbar\omega_D$ are excited with an equal probability), and the results are practically indistinguishable from the phonon-bubble initial condition (if one is interested in the thermalization time and dynamics of the energy contained in the electronic and phonon systems).

The third initial condition corresponds to an extreme case of a very high e-e relaxation rate, which, at all energies where $\epsilon < E_{\text{photon}}$, exceeds the e-ph relaxation rate and at $\epsilon \simeq k_B T$ is larger than $1/\tau_{|\Delta|}$. In this situation, electrons are thermalized at $t \ll \tau_{|\Delta|}$ and all of the energy of the photon is kept in the electronic system at $t = 0$,

$$n_\epsilon(t=0) = \frac{1}{e^{\epsilon/k_B T_e} + 1},$$
$$N_\epsilon(t=0) = N^{\text{eq}}. \tag{18}$$

In all cases, we choose parameters α, β, and T_e in Eqs. (16)–(18) in a way to keep the absorbed energy per unit of volume the same. For the electron-bubble condition, we choose $\epsilon_0 \gg \hbar\omega_D$, while, for the phonon-bubble condition, $\epsilon_0 \simeq \hbar\omega_D$.

During calculations, we check to see that the energy is conserved:

$$E_{\text{photon}}/V_{\text{init}} = (E_{\text{ph}} + E_e)/V_{\text{init}} - (E_{\text{ph}} + E_e)^{\text{eq}}/V_{\text{init}}, \tag{19}$$

where E_{ph} is the energy of the phonon system in the Debye model with a quadratic density of states $\mathcal{D}(\epsilon) = 9\epsilon^2/\hbar\omega_D$ per ion,

$$E_{\text{ph}}/V_{\text{init}} = \frac{1}{V_{\text{init}}} \frac{\mathcal{D}(\hbar\omega_D)}{\hbar(\hbar\omega_D)^2} \int_0^{\hbar\omega_D} \epsilon^3 N d\epsilon$$
$$= \frac{E_0}{\gamma} \int_0^{\hbar\omega_D/k_B T_c} \tilde{\epsilon}^3 N d\tilde{\epsilon}. \tag{20}$$

E_e is the energy of electrons (quasiparticles) in the superconductor,

$$E_e/V_{\text{init}} = 4N(0)\left\{ \int_0^\infty \epsilon N_1 n d\epsilon - \frac{|\Delta|^2}{4}\left[\frac{1}{2} + \ln\left(\frac{\Delta_0}{|\Delta|}\right)\right]\right\}$$
$$= E_0\left\{\int_0^\infty N_1 \tilde{\epsilon} n d\tilde{\epsilon} - \left(\frac{|\Delta|}{2k_B T_c}\right)^2\right.$$
$$\left. \times \left[\frac{1}{2} + \ln\left(\frac{\Delta_0}{|\Delta|}\right)\right]\right\}, \tag{21}$$

with $\tilde{\epsilon} = \epsilon/k_B T_c$, $\Delta_0 = 1.76k_B T_c$, and $E_0 = 4N(0)(k_B T_c)^2$.

In our numerical calculations, we use parameters typical for NbN: $\hbar\omega_D = 30$ meV (the chosen value of $\hbar\omega_D$ is a compromise among a variety of values known for different phases of NbN [15]), $k_B T_c = 0.86$ meV ($T_c = 10$ K),
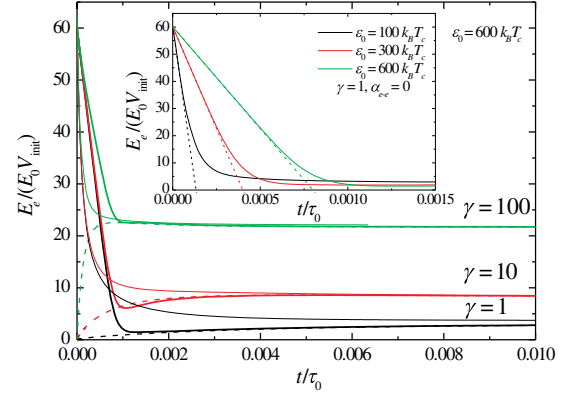
FIG. 1.   Dependence of the electronic energy E_e on the time found in a solution of kinetic equations at different γ's and different initial conditions: an electron bubble with $\epsilon_0 = 600k_B T_c$, $\alpha_{e\text{-}e} = 0$ (the solid thick curves), a phonon bubble with $\epsilon_0 = 30k_B T_c$, $\alpha_{e\text{-}e} = 0$ (the dashed curves), and hot electrons with the initial electronic temperature $T_e = 8.6T_c$, $\alpha_{e\text{-}e} = 1000$ (the solid thin curves). In all cases, the energy injected into the electrons and the phonons is the same and is equal to $\simeq 1.3$ eV in the volume $V_{\text{init}} = \pi\xi^2 d \simeq 290$ nm³. (Inset) The dynamics of E_e with an electron-bubble initial condition, $\alpha_{e\text{-}e} = 0$, and different ϵ_0's. The dashed lines indicate the linear dependence $E_e = E_{\text{photon}}(1 - t/\tau_{\text{leak}})$, with τ_{leak} taken from Eq. (22).

$T = T_c/2$, and $E_{\text{photon}}/E_0 V_{\text{init}} = 60$ [with $N(0) = 25.5$ eV⁻¹ nm⁻³ [16], $\xi = 4.8$ nm, and $d = 4$ nm, this value corresponds to $E_{\text{photon}} \simeq 1.3$ eV], and we neglect the escape of nonequilibrium phonons to the substrate because, usually, $\tau_{\text{esc}} \gg \tau_{|\Delta|}$.

When $t \lesssim \tau_{|\Delta|}$, energy of the absorbed photon of about 1.3 eV is concentrated at a relatively small volume, $V_{\text{init}} \simeq \pi\xi^2 d \simeq 290$ nm³, which indicates a high energy concentration. The larger the γ, the higher the temperature of both the electrons T_e and the phonons $T_{\text{ph}} = T_e$, as one can see from Eqs. (19)–(21) if one inserts Fermi-Dirac and Bose-Einstein functions in them for n_ϵ and N_ϵ, respectively (these functions nullify collision integrals when the down-conversion cascade is over and one neglects the diffusion of the electrons). Because the electron-phonon relaxation time $\tau_{e\text{-ph}}(\epsilon \ll k_B T_e) \simeq T_e^{-3}$ and $\tau_{e\text{-}e}(\epsilon \ll k_B T_e) \simeq \alpha_{e\text{-}e}^{-1} T_e^{-1}$, one can expect that, for a relatively large γ and $\alpha_{e\text{-}e}$, the energy of an optical or near-infrared photon can be shared between electron and phonon systems and electrons with phonons can be thermalized by the time $t \simeq \tau_{|\Delta|}$.

To prove it in Fig. 1, we show the time dependence of the energy of the electronic system calculated at different initial conditions, $\gamma = 1$–100, and at the same injected energy. One can see that, for $\gamma = 100$, by the time $\tau_{\text{sh}} \simeq 0.001\tau_0$, the largest part of the injected energy is already shared between electrons and phonons (even in the absence of e-e scattering), and τ_{sh} increases with a decrease of γ. Parameter γ controls what part of injected energy goes to electronic system—the larger γ is, the larger this part is (see Fig. 1).
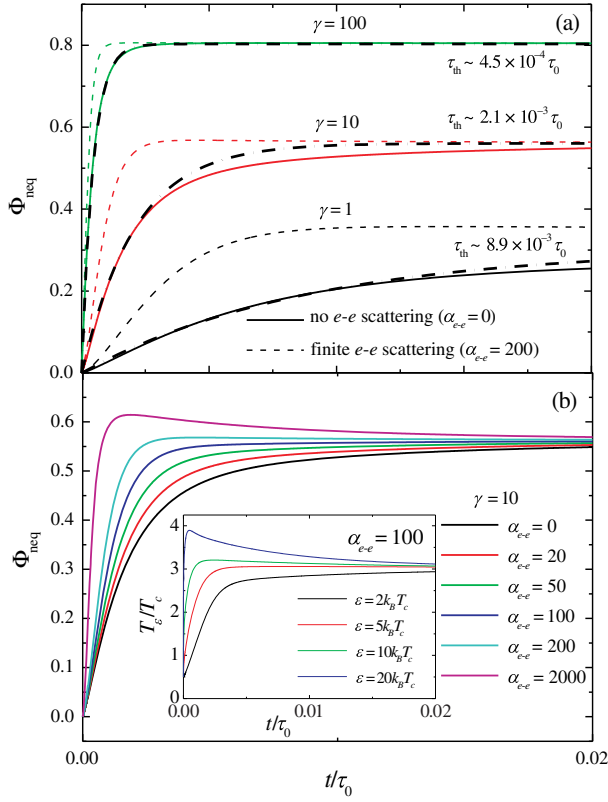
FIG. 2. (a) Time evolution of Φ_{neq} at different γ's and two values of $\alpha_{e\text{-}e}$. Fitting $\Phi_{neq}(t)$ (when $\alpha_{e\text{-}e} = 0$) with the expression $\Phi_{neq}(t \to \infty)[1 - \exp(-t/\tau_{th})]$ is shown by thick dashed curves with a corresponding τ_{th}. (b) Time evolution of Φ_{neq} at $\gamma = 10$ and different $\alpha_{e\text{-}e}$'s. All results are obtained for a phonon-bubble initial condition and $T = T_c/2$. (Inset) Time evolution of $T_\epsilon = \epsilon/k_B \ln(1/n_\epsilon - 1)$ at different energies and $\gamma = 10$, $\alpha_{e\text{-}e} = 100$. At $t = 0$, $n_\epsilon = n_\epsilon^{eq}$, and $T_\epsilon = T = T_c/2$ at all energies. After an injection of energy to the phonon system, n_ϵ deviates from equilibrium, which leads to different T_ϵ's. $T_\epsilon = T_e \simeq 3T_c$ at all energies when $t \gg \tau_{th} \simeq 1.2 \times 10^{-3}\tau_0$.

The sharing time, τ_{sh}, is actually the thermalization time, τ_{th}, in electronic and phonon systems. In Fig. 2, we show the time evolution of Φ_{neq} (which controls the suppression of $|\Delta|$) at different γ's and $\alpha_{e\text{-}e}$'s. Results are found for the case with the phonon-bubble initial condition. Φ_{neq} practically stops depending on time when the electrons are thermalized and n_ϵ is described by the Fermi-Dirac function. We fit numerically $\Phi_{neq}(t)$ with the expression $\Phi_{neq}(t \to \infty)[1 - \exp(-t/\tau_{th})]$ and find τ_{th} (examples of the fitting are shown in Fig. 2). One can see that thermalization time decreases with an increase of γ (which is a consequence of a larger energy transfer to an electron system) or an increase of $\alpha_{e\text{-}e}$ (which is a consequence of a shorter $\tau_{e\text{-}e}$).

In the case with an electron-bubble initial condition and $\epsilon_0 \gg \hbar\omega_D$, $\delta\epsilon \ll \epsilon_0$, one can find an analytical expression for the time τ_{leak} during which the energy leaks from electrons to phonons at the very beginning of the

down-conversion cascade. Indeed, inserting n_ϵ in the form of Eq. (16) into a phonon-electron collision integral, one finds that $I_{ph\text{-}e} \simeq 2\gamma\alpha/(\tau_0 k_B T_c)$ at energies where $\epsilon \gg |\Delta|$. Then, assuming that α depends on time and the full energy is conserved and is equal to the energy of the photon (we neglect here $E_e^{eq} + E_{ph}^{eq} \ll E_{photon}$), one finds that $E_e = E_{photon} \exp(-t/\tau_{leak})$, with

$$\tau_{leak} = \tau_0 \frac{2\epsilon_0(k_B T_c)^3}{(\hbar\omega_D)^4} = \frac{2\epsilon_0 \hbar}{g(\hbar\omega_D)^2}. \qquad (22)$$

At $t \ll \tau_{leak}$, one has the linear decay $E_e = E_{photon}(1 - t/\tau_{leak})$, which is shown as dashed lines in the inset of Fig. 1. For $\gamma = 100$, $\tau_{leak} \simeq \tau_{th}$ and the above simple calculations are valid only qualitatively. For $\gamma = 1$, 10, $\tau_{leak} \ll \tau_{th}$ and there is good quantitative agreement between the numerical and analytical results at $t \lesssim \tau_{leak}$ (see the inset in Fig. 1). When $\tau_{leak} \ll \tau_{th}$, the phonon system absorbs more energy by the time $t \simeq \tau_{leak}$ than it should have at $t \gg \tau_{th}$, according to the energy-conservation law [see Eqs. (19)–(21)], and it leads to nonmonotonic time dependence of E_e when $\gamma = 1$, 10 (this effect is absent for $\gamma = 100$ when $\tau_{leak} \simeq \tau_{th}$; see Fig. 1).

For self-consistency of the cited τ_{th}, the radius of the initial hot spot (ξ in our model) should coincide or be smaller than the diffusion length of the hot electrons, approximately $2\sqrt{D\tau_{th}}$. To make such a comparison, one should know τ_0, γ, and $\alpha_{e\text{-}e}$ for NbN. A theoretical estimation with the help of Eq. (6) and $g = 1$ gives $\tau_0 \simeq 925$ ps. τ_0 can also be found if one knows $\tau_{e\text{-}ph}(T_c)$ via the relation $\tau_0 = 14\zeta(3)\tau_{e\text{-}ph}(T_c)$ [9,17]. In thin NbN film $\tau_{e\text{-}ph}(T_c = 10 \text{ K}) \simeq 16$ ps [18], which gives us $\tau_0 \simeq 270$ ps. With the last value for τ_0 and $R_\square = 500 \ \Omega$, we find $\alpha_{e\text{-}e} \simeq 1.8$. Such a small $\alpha_{e\text{-}e}$ indicates that [see Fig. 2(b)], at least at the initial stage of hot-spot formation, e-e scattering plays a small role and down-conversion cascade and thermalization occurs mainly via electron-phonon and phonon-electron scattering. Our estimation of $\gamma = 9$ for NbN is based on $N_{ion} = 4.8 \times 10^{22}$ cm^{-3}, calculated with a molar mass of 106.9 g/mol and a density of $\rho = 8.47$ g/cm^3 [19]. Therefore, for NbN, $\tau_{th} \simeq 2.1 \times 10^{-3}\tau_0 \simeq 0.57$ ps $> \tau_{|\Delta|} \simeq 0.42$ ps and the radius of the initial hot spot is $2\sqrt{D\tau_{th}} \simeq 11$ nm, more than 2 times larger than $\xi = 4.8$ nm. These calculations show that one cannot expect complete thermalization of electrons and phonons in NbN by the time that the radius of the hot spot becomes about ξ and $E_{photon} = 1.3$ eV.

We also do calculations for WSi material, which demonstrate a good ability to detect single photons in the optical and near-infrared range [20]. We take the parameters of WSi from Ref. [21] [$T_c = 3.4$ K, $N(0) = 26.5$ eV/nm^3, $\hbar\omega_D = 34$ meV, $D = 0.58$ cm^2/s, $d = 3.4$ nm]. The results are shown in Fig. 3, where we use only the phonon-bubble initial condition and $\gamma = 100$,
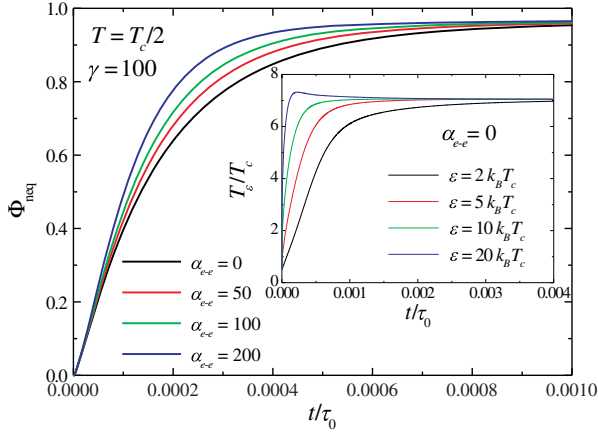
FIG. 3. Time evolution of Φ_{neq} at $\gamma = 100$ and for different $\alpha_{e\text{-}e}$'s. All results are obtained for the phonon-bubble initial condition, $T = T_c/2$, and the parameters of WSi taken from Ref. [21]. (Inset) Time evolution of $T_\epsilon = \epsilon/k_B \ln(1/n_\epsilon - 1)$ at different energies and $\alpha_{e\text{-}e} = 0$. After injection of energy to the phonon system, n_ϵ deviates from equilibrium, which leads to different T_ϵ's. $T_\epsilon = T_e \simeq 7T_c$ at all energies where $t \gg \tau_{\mathrm{th}} \simeq 1.9 \times 10^{-4}\tau_0$.

which is close to the $\gamma = 89$ expected for WSi ($C_e/C_{\mathrm{ph}}|_{T_c} = 5.65$ is calculated in Ref. [21] with the help of the molar mass and density of WSi). In this material, $\tau_0 \simeq 10$ ns if one uses the theoretical estimation from Ref. [21] or $\tau_0 \simeq 1.9$ ns, which follows from a recent experiment where $\tau_{e\text{-}ph}$ was extracted from the temperature dependence of magnetoconductivity [22]. We adopt the last value and, with $R_\square = 595\,\Omega$, it gives us $\alpha_{e\text{-}e} \simeq 5$. For $E_{\mathrm{photon}} = 1.3$ eV, we have $\tau_{\mathrm{th}} \simeq 1.9 \times 10^{-4}\tau_0 \simeq 0.36$ ps $\ll \tau_{|\Delta|} \sim 1.3$ ps for WSi, and the radius of the hot spot $2\sqrt{D\tau_{\mathrm{th}}} \simeq 9.1$ nm is close to the coherence length in WSi, $\xi \simeq 8.3$ nm, which we use when calculating V_{init}.

It seems that accounting for the diffusion of nonequilibrium electrons at the initial stage of hot-spot formation (at $t \lesssim \tau_{|\Delta|}$) should only decrease τ_{th}. Indeed, the volume of hot spot is $V \ll V_{\mathrm{init}}$ at times $t \ll \tau_{|\Delta|}$, which leads to a higher energy concentration and, hence, faster thermalization.

It is obvious that τ_{th} depends on the energy of the photon and V_{init}. This thermalization time can be estimated without solving the kinetic equations, with the help of the energy-conservation law [Eq. (19)] and if one associates τ_{th} with $\tau_{e\text{-}ph}(T_e)$ for electrons having the energy $\epsilon \ll k_B T_e$. Assuming that the electron and phonon distribution functions are described by Fermi-Dirac and Bose-Einstein expressions with $T = T_e = T_{\mathrm{ph}}$ from Eqs. (20) and (21), one finds Eqs. (24) and (25) from Sec. IV. For NbN and WSi materials, it follows from Eqs. (19), (24), and (25) that the absorption of a photon with the energy 1.3 eV in a chosen volume $V_{\mathrm{init}} = \pi\xi^2 d$ heats locally electrons and phonons up to the temperatures $T_e = T_{\mathrm{ph}} \simeq 3T_c$ and $T_e = T_{\mathrm{ph}} \simeq 7T_c$, respectively, which is close to the results of the numerical calculations [see the insets in Figs. 2(b)

and 3]. $\tau_{e\text{-}ph}(T_e)$ can be expressed via τ_0 as $\tau_{e\text{-}ph}(T_e) = \tau_0/[14\zeta(3)](T_c/T_e)^3$ [9,17], which gives $\tau_{\mathrm{th}} = \tau_{e\text{-}ph}(T_e) \simeq 2.2 \times 10^{-3}\tau_0$ and $1.8 \times 10^{-4}\tau_0$ for these materials, which is again close to the numerical results.

We make the same calculations for normal metal (we put $|\Delta| = 0$, which in the experiment can be done with the application of a relatively large magnetic field) and get very similar results. This finding is not surprising because, at times where $t \ll \tau_{\mathrm{leak}}$, deviation from equilibrium occurs at energies much larger than $|\Delta|$, while, when $t > \tau_{\mathrm{th}}$, the main contribution to the collision integrals comes from energies $\epsilon \simeq k_B T_e \gg |\Delta| \simeq 1.76k_B T_c$ (see the insets in Figs. 2 and 3), where the spectral functions N_1 and R_2 are close to their values in the normal state. We also expect weak dependence on the bath temperature (if it varies in the range $0 \lesssim T \lesssim T_c$) because of large injected energy, which provides local heating of electrons and phonons up to $T_e \gg T_c$.

We have to stress that our results are valid only at $t \lesssim \tau_{|\Delta|}$, when the volume of the hot spot is smaller than $V_{\mathrm{init}} = \pi\xi^2 d$. At larger times, $t \gtrsim \tau_{|\Delta|}$, shown in Figs. 1–3, the results should be considered as only a precursor for the consequent dynamics of E_e and Φ_{neq}. To study the evolution of a hot spot at $t \gtrsim \tau_{|\Delta|}$, we consider two limits. In the first limit, with the long thermalization time $\tau_{\mathrm{th}} \sim \tau_{D,w} \gg \tau_{|\Delta|}$ ($\tau_{D,w} \simeq w^2/16D - w^2/4D \simeq 12.5$–50 ps for a strip with $w = 100$ nm and $D = 0.5$ cm^2/s, depending on where the photon is absorbed—in the center or at the edge of the strip), it is assumed that the largest impact on superconducting properties occurs when hot electrons reach both edges of the strip and simultaneously become thermalized. We expect such a situation in superconductors with a small D ($\lesssim 1$ cm^2/s) and $\gamma \leq 1$, or in materials with a relatively large γ (>1) and a large diffusion coefficient, $D \gg 1$ cm^2/s. Because, usually, $\tau_{D,w} \gg \tau_{|\Delta|}$, we expect that $|\Delta|(t)$ changes with $\Phi_{\mathrm{neq}}(t)$ instantly and, by the time that $t \simeq \tau_{D,w}$, one has a hot belt—a region with heated electrons and phonons up to a temperature of $T_e = T_{\mathrm{ph}} > T$ and a partially suppressed $|\Delta|(T_e)$ across the entire width of the strip [see Fig. 4(a)]. To calculate T_e and to find the critical current of the strip with a hot belt, one can use the energy-conservation law. This problem is considered in Sec. IV.

In the second limit, with the short thermalization time $\tau_{\mathrm{th}} \lesssim \tau_{|\Delta|}$, Φ_{neq} already reaches its maximal value a short time after the energy injection (see Fig. 2) with a radius of the hot spot $R_{\mathrm{hs}} \sim \xi \ll w$ [we expect that it is realized in superconductors with relatively small D ($\lesssim 1$ cm^2/s) and a large γ ($\gtrsim 100$)]. Because of the diffusion of electrons, T_e decreases (and Φ_{neq} decreases, too) inside the hot spot but, while $T_e > T_c$ and $R_{\mathrm{hs}} \gg \xi$, the order parameter in the hot region is strongly suppressed. It provides a large current-crowding effect around the hot spot (the superconducting
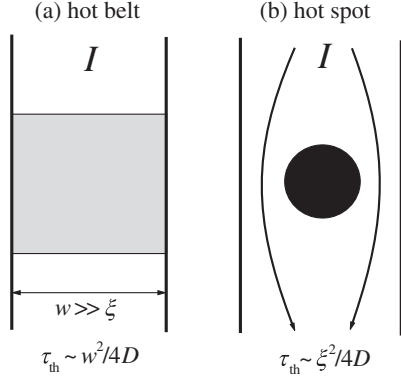
FIG. 4. (a) In material with relatively large thermalization time $\tau_{\mathrm{th}} \sim w^2/4D$ the superconducting state becomes unstable when photon induced hot electrons form hot belt (weak link) in the strip. (b) In material with short thermalization time $\tau_{\mathrm{th}} \sim \xi^2/4D$ the superconducting state becomes unstable, due to current crowding effect, before the hot electrons reach both edges of the strip.

current avoids the region with a suppressed Δ), and the current-carrying state may become unstable before hot electrons reach both edges of the strip [this situation is shown in Fig. 4(b)]. We study the dynamics of Δ in this limit using modified time-dependent Ginzburg-Landau equation. We also introduce the effective temperature of the electrons and phonons and solve heat-conduction equations instead of Eqs. (1) and (2). This limit is studied in Sec. V.

IV. HOT-BELT MODEL

In the hot-belt model, we assume that hot electrons are thermalized among themselves and with phonons by the time that they reach the edges of the strip and form a hot belt with a size of about $w \times w$ and with a local temperature of $T_e = T_{\mathrm{ph}} > T$. As a result, the critical current of the strip becomes equal to $I_c(T_e)$ because usually $w \gg \xi$ and the proximity effect from the regions next to the belt, where $|\Delta|(T) > |\Delta|(T_e)$, can be neglected. We also assume that the escape time of nonequilibrium phonons to substrate is $\tau_{\mathrm{esc}} \gg \tau_{D,w}$. The effective temperature T_e may be determined at a given bath temperature T and energy of the photon from the energy-conservation law

$$\frac{E_{\mathrm{photon}}}{E_0 w^2 d} = [\mathcal{E}_e(T_e) + \mathcal{E}_{\mathrm{ph}}(T_e)] - [\mathcal{E}_e(T) + \mathcal{E}_{\mathrm{ph}}(T)], \quad (23)$$

where $\mathcal{E}_{\mathrm{ph}}(T)$ is the dimensionless energy of the phonon system per unit of volume,

$$\mathcal{E}_{\mathrm{ph}}(T) = \frac{1}{\gamma} \int_0^{\hbar\omega_D/k_B T_c} \tilde{\epsilon}^3 N_{\tilde{\epsilon}} d\tilde{\epsilon} = \frac{1}{\gamma} \frac{\pi^4}{15} \left(\frac{T}{T_c}\right)^4 \quad (24)$$

(where $\hbar\omega_D/k_B T_c \gg 1$ and $N_{\tilde{\epsilon}}$ is described by the Bose-Einstein function). In Eq. (23), $\mathcal{E}_e(T)$ is the dimensionless electronic energy per unit of volume,

$$\mathcal{E}_e(T) = \int_{|\Delta|/k_B T_c}^{\infty} \tilde{\epsilon} N_1 n_{\tilde{\epsilon}} d\tilde{\epsilon}$$

$$- \left(\frac{|\Delta|}{2k_B T_c}\right)^2 \left[\frac{1}{2} + \ln\left(\frac{\Delta_0}{|\Delta|}\right)\right]$$

$$= \frac{\pi^2}{12} \left(\frac{T}{T_c}\right)^2 - \mathcal{E}_s(T), \quad (25)$$

where $n_{\tilde{\epsilon}}$ is described by the Fermi-Dirac function. For N_1, we use Eq. (13) and

$$\mathcal{E}_s(T) = \int_0^{|\Delta|/k_B T_c} \tilde{\epsilon} n_{\tilde{\epsilon}} d\tilde{\epsilon} - \int_{|\Delta|/k_B T_c}^{\infty} \tilde{\epsilon}(N_1 - 1) n_{\tilde{\epsilon}} d\tilde{\epsilon}$$

$$+ \left(\frac{|\Delta|}{2k_B T_c}\right)^2 \left[\frac{1}{2} + \ln\left(\frac{\Delta_0}{|\Delta|}\right)\right] \quad (26)$$

is the gain in the energy of the electrons due to their transition to the superconducting state at $T < T_c$ [$\mathcal{E}_s(T) = 0$ at $T > T_c$].

For practical purposes, one may use the following interpolation expressions for $\mathcal{E}_s(T)$ and $|\Delta|(T)$:

$$\mathcal{E}_s(T) = \left(\frac{|\Delta|(T)}{2k_B T_c}\right)^2 \left[1 - 0.053\left(\frac{|\Delta|(T)}{k_B T_c}\right)^2\right.$$

$$\left. - 0.1\left(\frac{|\Delta|(T)}{\Delta_0}\right)^4 - 0.236 e^{-12[1 - |\Delta|(T)/\Delta_0]^{0.7}}\right], \quad (27)$$

$$|\Delta|(T) = 1.76 k_B T_c \tanh(1.74\sqrt{T_c/T - 1}), \quad (28)$$

which satisfy Eqs. (9), (10), and (26) with an accuracy better than 2%. Note that the maximal value of $\mathcal{E}_s$ is reached at about $T = T_c/2$, where $\mathcal{E}_s^{\max} \simeq 1/2$.

In the presence of the superconducting current, $\mathcal{E}_s$ decreases with a maximal change at $I = I_{\mathrm{dep}}(T)$. This effect can be taken into account only numerically, and it leads to small quantitative differences from the results presented in Figs. 5 and 6. We neglect it here.

To calculate at which threshold (we call it detection I_{det}) current the photon drives the superconducting strip to the resistive state, one needs to know the temperature-dependent critical current, which is equal to $I_{\mathrm{dep}}(T_e)$ in our model. For simplicity, we adopt the Bardeen expression

$$I_{\mathrm{det}} = I_{\mathrm{dep}}(T_e) = I_{\mathrm{dep}}(0) \left[1 - \left(\frac{T_e}{T_c}\right)^2\right]^{3/2}. \quad (29)$$

With Eqs. (23)–(29), it is easy to determine how the detection current changes with the photon's energy at a given T and γ. Examples of these dependencies are shown in Fig. 5. With an increasing γ, detection current drastically decreases and, at large γ, practically does not depend on it because almost all energy of the photon goes to an electronic system when $\gamma \gg 1$. At $\gamma \lesssim 1$, only a small
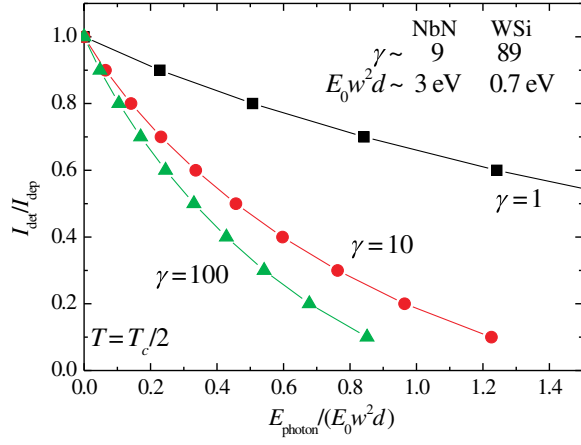
FIG. 5. Dependence of the detection current on the photon's energy at different γ's and bath temperature $T = T_c/2$ calculated in a hot-belt model with the help of Eqs. (23)–(29). (Inset) The expected γ's and $E_0 w^2 d$'s for NbN- and WSi-based detectors (with $d = 4$ nm, $w = 100$ nm, and $d = 3.4$ nm, and $w = 150$ nm, respectively).

fraction of the photon's energy goes to the electronic system, and the detection current is about I_{dep} for the considered photon's energies.

If we fix the $I/I_{\mathrm{dep}}(T)$ ratio, the energy of the photon E_{photon}, whose absorption drives the superconducting strip to the resistive state, changes nonmonotonically with temperature (see Fig. 6). The nature of the effect can be easily understood with the help of Fig. 7. In this figure, we present $I_{\mathrm{dep}}(T)$ (the solid curve) and show how much one should increase the temperature (by δT) in the hot belt to transfer the strip to the resistive state at three different temperatures and $I/I_{\mathrm{dep}}(T) = 0.5$. δT decreases with an increase of T but, due to the nonlinear temperature dependencies $\mathcal{E}_e(T)$ and $\mathcal{E}_{\mathrm{ph}}(T)$, heating the strip from
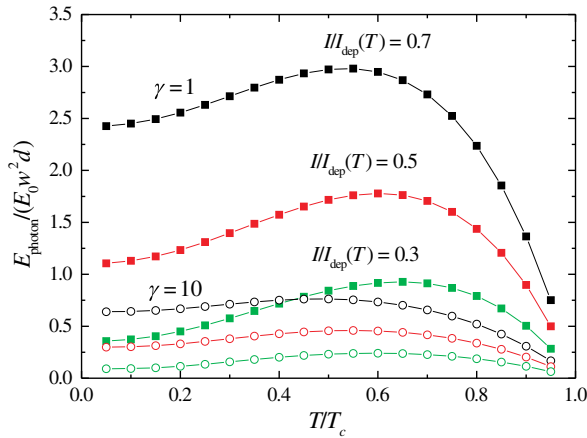
FIG. 6. Dependence of energy of the photon E_{photon}, whose absorption drives the superconducting strip to the resistive state, on temperature for $I/I_{\mathrm{dep}}(T) = 0.3, 0.5, 0.7$ and $\gamma = 1, 10$. Calculations are made in the framework of the hot-belt model.
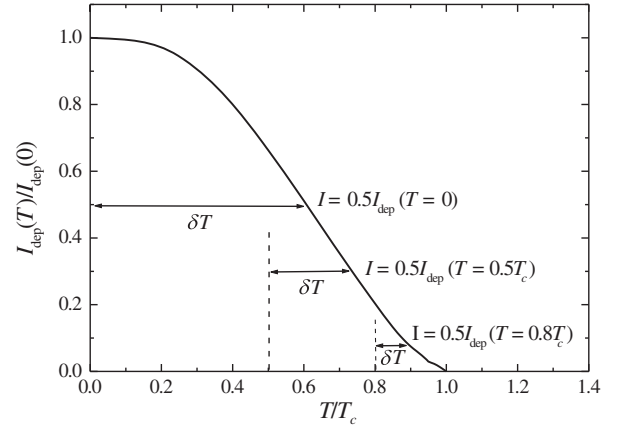
FIG. 7. Depiction of how much one should increase the temperature in the hot-belt region [at three different bath temperatures, $T = 0, 0.5T_c, 0.8T_c$, and three currents, $I = I_{\mathrm{dep}}(T)/2$] to drive the superconducting strip to the resistive state.

$T = 0.5T_c$ up to $0.74T_c$ takes more energy than it does from $T = 0$ up to $0.61T_c$. Because $\delta T \to 0$ as $T \to T_c$, there is a local maxima in dependence $E_{\mathrm{photon}}(T)$ (the position of the maxima depends on γ and I/I_{dep}; see Fig. 6).

In the above consideration, we assume that, at $I > I_{\mathrm{det}}$, expanding the normal domain appears in the superconducting strip, which leads to a relatively large voltage signal in a contemporary superconducting nanowire single-photon detector (SNSPD). It is well known that, below some retrapping current $I_r(T)$, the normal domain cannot expand and shrinks in the current-carrying strip [23,24]. Therefore, to see the voltage signal in existing SNSPDs, the current in the strip should at least exceed I_r. Thus, for relatively large photon energies I_{det} should be about $I_r(T)$ and does not depend on E_{photon}. Support for this idea can be found in Ref. [25], where WSi-based SNSPDs were studied. In Fig. 3(a) of that work, the dependence of the photon detection efficiency (DE) on the current is present at different temperatures. One can see that, in a wide temperature interval, DE starts to increase at the current which weakly depends on the temperature. This phenomena resembles weak temperature dependence of I_r at relatively low temperatures [see, for example, Fig. 7(b) in Ref. [24]], in contrast to the noticeable temperature dependence of the critical (switching) current in the same temperature interval [compare Fig. 3(a) of Ref. [25] to Fig. 7(b) of Ref. [24]].

For the same reason, one should treat the results shown in Fig. 6 carefully at temperatures close to T_c. As $T \to T_c$, the retrapping current approaches the depairing (critical) current and at a certain temperature where $I_r = I_{\mathrm{dep}}$ (in Ref. [24], it occurs at $T \simeq 0.82T_c$). Therefore, the results presented in Fig. 6 are valid when the current is larger than $I_r(T)$.

Let us make estimations for NbN and WSi. $E_0 w^2 d \simeq 3$ eV and $\gamma \sim 9$ in the case of a NbN strip with $w = 100$ nm and $d = 4$ nm. For WSi strip $E_0 w^2 d \simeq 0.7$ eV and $\gamma \sim 89$

($w = 150$ nm, $d = 3.4$ nm). According to Fig. 5 at current $I = I_{\text{dep}}/2$ and temperature $T = T_c/2$ NbN strip would be able to detect single photons with energy 1.35 eV, while a WSi strip can detect photons with a much smaller energy 0.23 eV, if one believes that the hot-belt model is valid for these materials and $\tau_{\text{esc}} \gg \tau_{D,w}$.

V. HOT-SPOT TWO-TEMPERATURE MODEL

In this section, we study a limiting case with a short thermalization time $\tau_{\text{th}} \simeq \tau_{|\Delta|}$ at the initial stage of hot-spot formation. Because of the diffusion of hot electrons (one may neglect the diffusion of hot phonons due to their much lower group velocity compared to the one for electrons), concentration of the absorbed photon's energy in a hot spot with a radius $R_{\text{hs}} > d$ decreases as $1/R_{\text{hs}}^2$. However, because $\mathcal{E}_e \sim T_e^2$ [see Eq. (25)] and $\mathcal{E}_{\text{ph}} \sim T_{\text{ph}}^4$ [see Eq. (24)], the temperature of the electrons drops under about $1/R_{\text{hs}}$. One also should keep in mind that, with a decrease of T_e and T_{ph}, the major part of the photon's energy goes to the electronic system due to a faster decrease of $\mathcal{E}_{\text{ph}}$ than in $\mathcal{E}_e$.

Because, the diffusion time $\tau_D \sim R_{\text{hs}}^2/4D$ rapidly increases, one can expect that during diffusion the non-equilibrium electrons have time for their thermalization and that the electron distribution function can be described by the Fermi-Dirac function with an effective temperature $T_e \neq T$. Indeed, when $T_e \simeq T_c$, the diffusion of hot electrons is impeded due to a large $|\Delta|$ ($\simeq \Delta_0 \simeq 1.76 k_B T_c$) outside the hot spot, which should favor the thermalization of electrons.

In NbN, electrons and phonons are not thermalized on time scales $\lesssim \xi^2/4D$ (see Sec. III). However, the difference between diffusion time and thermalization time is not huge and one can expect that, despite an absence of full thermalization, Φ_{neq} is relatively strong inside the growing hot spot and is sufficient to suppress $|\Delta|$ substantially. Indirect prove of this idea comes from the experiment with a magnetic field [26] which validates the hot-spot model with a strongly suppressed Δ in this material. From a quantitative point of view, usage of the two-temperature (2T) model for NbN leads to a smaller value for the detection current (at a fixed energy of the photon) due to the stronger suppression of $|\Delta|$ inside the hot spot than when the electrons are not fully thermalized.

In the absence of phonon-phonon interaction, thermalization of the phonons occurs only via electron-phonon and phonon-electron scattering. Our study of the initial stage of hot-spot formation demonstrates the dependence of the dynamics of Φ_{neq} only on the value of the injected energy to the phonon system, not on the method of injection (phonon-bubble or phonon-plateau initial conditions). To account for the energy adopted by the phonon system during the diffusion of electrons, we assume that the phonon distribution function is described by the Bose-Einstein expression with a phonon temperature T_{ph}, which, in general, can be different from T_e.

With the above assumptions from Eqs. (1)–(4), one can derive (as was done in Ref. [27] for a normal metal) equations for the dynamics of electron and phonon temperatures,

$$\frac{\partial}{\partial t}\left(\frac{\pi^2 k_B^2 N(0) T_e^2}{3} - E_0 \mathcal{E}_s(T_e, |\Delta|)\right)$$
$$= \nabla k_s \nabla T_e - \frac{96\zeta(5) N(0) k_B^2}{\tau_0} \frac{T_e^5 - T_{\text{ph}}^5}{T_c^3} + \vec{j}\vec{E}, \quad (30)$$

$$\frac{\partial T_{\text{ph}}^4}{\partial t} = -\frac{T_{\text{ph}}^4 - T^4}{\tau_{\text{esc}}} + \gamma \frac{24\zeta(5)}{\tau_0} \frac{15}{\pi^4} \frac{T_e^5 - T_{\text{ph}}^5}{T_c}, \quad (31)$$

where k_s is the heat conductivity in the superconducting state,

$$k_s = k_n\left(1 - \frac{6}{\pi^2 (k_B T_e)^3}\int_0^{|\Delta|} \frac{\epsilon^2 e^{\epsilon/k_B T_e} d\epsilon}{(e^{\epsilon/k_B T_e} + 1)^2}\right). \quad (32)$$

$k_n = 2D\pi^2 k_B^2 N(0) T_e/3$ is the heat conductivity in the normal state, and the last term in Eq. (30) describes the Joule dissipation ($\vec{j}$ is the current density and $\vec{E}$ is an electric field).

Note that, when both $|\Delta|$ and T_e vary on a time scale comparable to $\tau_{|\Delta|}$, $|\Delta|$ is not determined by T_e via Eq. (10) or (27), and for $\mathcal{E}_s$ in Eq. (30), one has to use Eq. (26) with the independent time-dependent variables $T_e(t)$ and $|\Delta|(t)$. As a physical consequence, variation of $|\Delta|$ leads to the heating or cooling of electrons [28], depending on the sign of $\partial|\Delta|/\partial t$.

For the derivation of Eqs. (30)–(32) we use Eqs. (13) and (14) for N_1 and R_2 and we put $M = 1$ into $I_{e\text{-ph}}$ and $I_{\text{ph-}e}$, which is strictly valid when $|\Delta| = 0$. In the superconducting state, $M \neq 1$, which leads to an increase of $\tau_{e\text{-ph}}$ and, hence, the process of the cooling of electrons via their coupling with phonons becomes longer. However, because the cooling of electrons is faster due to diffusion [usually, $\tau_{e\text{-ph}}(T_c) > \tau_{D,w}$], we do not expect a large influence for this effect, at least on a time scale $t < \tau_{D,w}$.

For a normal metal with $T_{\text{ph}} = T$, Eq. (30) was obtained in Refs. [27,29] and, in the limit $|T_{e,\text{ph}} - T| \ll T$, the above equations with zero-gradient terms coincide with Eqs. (13) and (14) in Ref. [30].

Appearance of the hot spot (the region with a suppressed $|\Delta|$) in the strip leads to current redistribution. To find the current distribution in each moment in time, one has to solve equation $\text{div}\vec{j} = 0$, where the current density $\vec{j} = \vec{j}_s + \vec{j}_n$ consists, in general, of superconducting $\vec{j}_s$ and normal $\vec{j}_n$ parts. The superconducting current in the dirty (Usadel) limit is described by the following expression:

$$\vec{j}_s^{Us} = \frac{\sigma_n}{e\hbar} \vec{q}_s \int_0^\infty 2N_2R_2(1-2n_\epsilon)d\epsilon$$
$$\simeq \frac{\pi\sigma_n}{2e\hbar} |\Delta| \tanh\left(\frac{|\Delta|}{2k_BT_e}\right)\vec{q}_s, \qquad (33)$$

where $\sigma_n = 2e^2DN(0)$ is the normal-state conductivity.

The last expression in Eq. (33) is obtained in the limit of a small $|q_s|$ ($\ll q_s^{dep}$), omitting the spatial derivative in Eq. (9) [in this case, $2N_2R_2 = \pi\delta(\epsilon - |\Delta|)/2$, where $\delta(x)$ is the Dirac function] and when, for n_ϵ, one uses the Fermi-Dirac function. It turns out that this expression gives a good approximation for $\vec{j}_s^{Us}$ at all $|q_s|$'s and we use it in our calculations. When $k_BT_e \gg |\Delta|$, from Eq. (33), one can derive a well-known expression for j_s in the Ginzburg-Landau model,

$$\vec{j}_s^{GL} = \frac{\pi\sigma_n|\Delta|^2}{4ek_BT_c\hbar}\vec{q}_s. \qquad (34)$$

For the normal component of the current density, we adopt the simplified expression

$$\vec{j}_n = -\sigma_n\nabla\varphi \qquad (35)$$

(φ is the electrostatic potential), which follows from a more general expression (see, for example, Refs. [31,32]) in the limit $k_BT_e \gg |\Delta|$. Note that the normal current density has a large value (comparable to or larger than j_s) only in the region with a suppressed $|\Delta|$, which confirms our choice.

To calculate the effect of $n_e \neq n_e^{eq}$ or $T_e \neq T$ on $|\Delta|$, we use a modified time-dependent Ginzburg-Landau equation which describes the dynamics of the complex order parameter $\Delta = |\Delta|e^{i\phi}$. Equation (10) is not convenient for studying the situation when a vortex (or vortices) appears in the superconducting system because, strictly in the center of the vortex $|\Delta| = 0$, $|\vec{q}_s| = \infty$ and there is a nonzero vorticity $\oint \nabla\phi dl = \pm 2\pi$ (+ for vortex and − for antivortex). It is more convenient to deal with an equation which operates with a complex order parameter where vortices appear naturally. Unfortunately, the usual Ginzburg-Landau (GL) equation is quantitatively valid only near T_c. Therefore, we modify the coefficients at the spatial derivative and at the nonlinear term ($\Delta|\Delta|^2$) in the GL equation to have the temperature dependence $|\Delta|(T)$ and $\xi(T)$ close to correct at all temperatures,

$$\frac{\pi\hbar}{8k_BT_c}\left(\frac{\partial}{\partial t} + \frac{2ie\varphi}{\hbar}\right)\Delta$$
$$= \xi_{mod}^2\left(\nabla - i\frac{2e}{\hbar c}A\right)^2\Delta + \left(1 - \frac{T_e}{T_c} - \frac{|\Delta|^2}{\Delta_{mod}^2}\right)\Delta$$
$$+ i\frac{(div\vec{j}_s^{Us} - div\vec{j}_s^{GL})}{|\Delta|}\frac{\hbar D}{\sigma_n\sqrt{2}\sqrt{1+T_e/T_c}}, \qquad (36)$$

where $\xi_{mod}^2 = \pi\sqrt{2}\hbar D/(8k_BT_c\sqrt{1+T_e/T_c})$, $\Delta_{mod}^2 = [\Delta_0\tanh(1.74\sqrt{T_c/T_e - 1})]^2/(1 - T_e/T_c)$, and A is the

vector potential. When $T_e \to T_c$, the coefficients ξ_{mod}^2 and Δ_{mod}^2 go to familiar GL coefficients in the dirty limit. We check to see that Eqs. (36) and (33) give the depairing current close to the one which follows from the dirty limit at all temperatures (the largest deviation $< 5\%$ occurs at $T = 0$), in contrast to the Ginzburg-Landau depairing current. The last term on the right-hand side of Eq. (36) provides a conservation of the superconducting current in the stationary state with $\dot\phi + 2e\varphi/\hbar = 0$: $div\vec{j}_s^{Us} = 0$. If we do not include this term, the stationary solution of Eq. (36) leads to $div\vec{j}_s^{GL} = 0$. The presence of hot electrons is reflected in Eq. (36) by $T_e \neq T$, whose effect on $|\Delta|$ is analogical to the effect of $\Phi_{neq} \neq 0$ in Eq. (10).

In the framework of the considered model, the electrostatic potential should be found from the current conservation law,

$$div\vec{j}_n = -\sigma_n\nabla^2\varphi = -div\vec{j}_s^{Us}. \qquad (37)$$

Equations (30), (31), (36), and (37) are solved numerically for a 2D superconducting strip of finite width $w = 20\xi_c$ and length $L = 4w = 80\xi_c$. $\xi_c^2 = \hbar D/k_BT_c \simeq 1.8\xi_{mod}^2(T_e = 0)$ is a natural length scale in the Usadel equation when the energy is scaled in units of k_BT_c, and we keep it for a modified GL equation, too. At the transverse edges, we use the boundary conditions $\vec{j}_n|_n = \vec{j}_s|_n = 0$ and $\partial T_e/\partial n = 0$, $\partial|\Delta|/\partial n = 0$, while, at the longitudinal edges, $T_e = T$, $|\Delta| = 0$, $\vec{j}_s|_n = 0$, $\vec{j}_n|_n = I/wd$. The latter boundary conditions model contact of the superconducting strip with a normal reservoir in equilibrium. This choice is not explained by any physical reason, but it is connected with the simplest way "to inject" the current into the superconducting strip in numerical modeling.

In numerical calculations, we scale the time in units $\tau_{T_c} = \hbar/k_BT_c$, which is proportional to $\tau_{|\Delta|}$ at low temperatures. We choose $\tau_0 = 900$ ps $\simeq 1184\tau_{T_c}$, which corresponds to our theoretical estimation for NbN with $T_c = 10$ K (see the discussion in Sec. III). We check to see that the results change slightly with an increase or decrease of τ_0 because main cooling of the hot electrons is due to their diffusion and not their coupling to the phonons (which is controlled by τ_0), at least at times $t \lesssim w^2/4D$.

Based on the results of Sec. III, we assume that, after absorption of the photon by the strip, the hot spot with size $2\xi_c \times 2\xi_c$ appears with $T_{e,ph} = T_{init} > T$ inside the hot spot and $T_{e,ph} = T$ outside it, while $|\Delta| = |\Delta|(T)$ everywhere. With this initial condition at $t = 0$, we study the dynamics of Δ and $T_{e,ph}$ in the strip. In our calculations, we put $\tau_{esc} = \infty$ (the effect of a finite τ_{esc} is discussed in Sec. VI).

We find that, for any $T_{init} > T$, there is a threshold current (we call it a detection current, I_{det}) above which the normal domain nucleates and expands in the strip after the appearance of the initial hot spot. The mechanism of destruction of the superconductivity depends on the
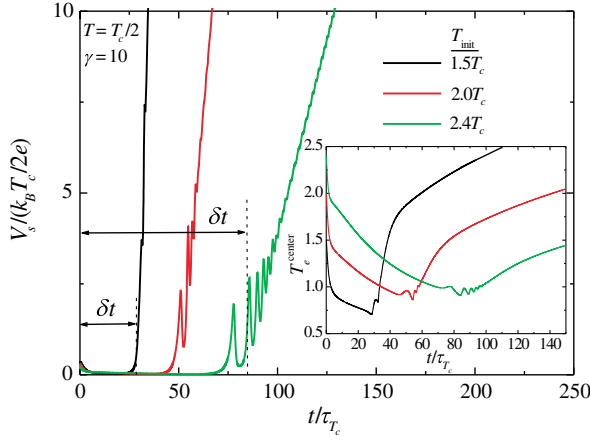
FIG. 8. Time dependence of the voltage along the superconducting strip V_s and the electron temperature in the center of the hot spot T_e^{center} (see the inset) calculated for different T_{init}'s. At $t = 0$, the initial hot spot appears in the center of the strip and I is slightly larger than I_{det} for a corresponding T_{init} (see Fig. 9). At $t \gtrsim \delta t$, there is rapid growth of the voltage because of expansion of the normal domain. Oscillations in V_s and T_e^{center} are connected with nucleation and the passage of vortices and antivortices across the strip.

FIG. 9. Dependence of I_{det} (at $I > I_{\mathrm{det}}$, the normal domain expands in the superconducting strip) and I_{vort} (at $I_{\mathrm{vort}} < I < I_{\mathrm{det}}$, the nucleation and the motion of the vortices do not lead to the appearance of a growing normal domain) on the coordinate of the initial hot spot having the size $2\xi_c \times 2\xi_c$ and different T_{init}'s. $T_{\mathrm{init}} = 1.5T_c$ corresponds to absorption of the photon with the energy $E_{\mathrm{photon}} \simeq 30.5E_0\xi_c^2 d \simeq 0.38$ eV, ($T_{\mathrm{init}} = 2.0T_c \rightarrow E_{\mathrm{photon}} \simeq 83.8E_0\xi_c^2 d \simeq 1.04$ eV, $T_{\mathrm{init}} = 2.4T_c \rightarrow E_{\mathrm{photon}} \simeq 162E_0\xi_c^2 d \simeq 2.0$ eV) by a NbN strip with the parameters used in Sec. III.

position of the initial hot spot in the strip. When it is located near the edge, at some stage of the hot-spot evolution (expansion), the vortex enters the region with a suppressed $|\Delta|$ from the nearest edge of the strip and passes through the superconductor. After that, the second, third, and succeeding vortices pass through the strip, and the electrons are heated because of the presence of electric field $\vec{E}$ and diffuse along the strip, which leads to expansion of the normal domain in the superconductor. When the initial hot spot is located near the center of the strip, the vortex and antivortex nucleate *inside* the expanding hot spot and move to opposite edges of the strip and, at $I > I_{\mathrm{det}}$, the normal domain again spreads in the strip. The time evolution of the voltage drop along the strip and the electronic temperature in the center of hot spot located in the center of the strip are shown in Fig. 8 for photons with different energies (different T_{init}'s) and at a current slightly above $I_{\mathrm{det}}(T_{\mathrm{init}})$.

Note that the moving vortices can be nucleated in the strip with a hot spot at a smaller current, $I = I_{\mathrm{vort}} < I_{\mathrm{det}}$, but their motion does not lead to the appearance of the growing normal domain when $I_{\mathrm{det}} \ll I_{\mathrm{dep}}$. Instead, after the passage of one or several vortices (the number of vortices depends on the current), the superconductivity recovers in the strip. This recovery occurs because, in the range of the currents $I_{\mathrm{vort}} < I < I_{\mathrm{det}}$, cooling of the hot electrons due to their diffusion outside the moving vortex core (where $|\vec{E}|$ is maximal) is not compensated for by their heating due to Joule dissipation, $\vec{j}\vec{E} \sim I^2$.

The dependence of both I_{vort} and I_{det} on the coordinate of the initial hot spot and different T_{init}'s is present in Fig. 9 (for material with $\gamma = 10$). This result qualitatively

coincides with the one found in the quasistationary hot-spot model (where the present I_{vort} was defined as I_{det}) [5,26] and resembles the experimental result in Ref. [33] [in Ref. [6], the nonmonotonic dependence $I_{\mathrm{det}}(y)$ was predicted, but without two local minima near the edges and, in that model, vortices enter the strip only via the edges]. Neither in Refs. [5,26] nor in Ref. [6] has the heating of the superconductor due to vortex motion or the condition for the appearance of the normal domain been studied.

As is discussed in Ref. [5], dependence $I_{\mathrm{det}}(y)$ explains the monotonic dependence of the detection efficiency of the SNSPD on the current [when it changes from its minimal, I_{det} ($I_{\mathrm{det}}^{\mathrm{min}}$), up to its maximal value, $I_{\mathrm{det}}^{\mathrm{max}}$]. It is interesting to note that the difference, $I_{\mathrm{det}}^{\mathrm{max}} - I_{\mathrm{det}}^{\mathrm{min}}$, decreases with an increase of T_{init} (the energy of the photon), which resembles the experimental results found for detectors based on WSi (see Fig. 2 in Ref. [20]), NbN (see Fig. 1 in Ref. [26]), and MoSi (see Figs. 2 and 4 in Ref. [34]). If one does not take into account the heating effects and associates I_{det} with I_{vort}, then $I_{\mathrm{det}}^{\mathrm{max}} - I_{\mathrm{det}}^{\mathrm{min}} = I_{\mathrm{vort}}^{\mathrm{max}} - I_{\mathrm{vort}}^{\mathrm{min}}$ increases with an increase of the energy of the photon (see Fig. 9 here or Fig. 5 in Ref. [5]).

When $I > I_{\mathrm{det}}^{\mathrm{max}}$, the detection efficiency reaches its maximal value [5]. $I_{\mathrm{det}}^{\mathrm{max}}$ is located either in the center of the strip or at its edge, depending on T_{init} (see Fig. 9 and compare it to Fig. 5 in Ref. [26] and Fig. 4 in Ref. [5]). In Fig. 10, we show the dependence of $I_{\mathrm{det}}^{\mathrm{max}}$ on the energy of the photon. Qualitatively, Fig. 10 resembles the results shown in Fig. 5 for the hot-belt model, but with one important
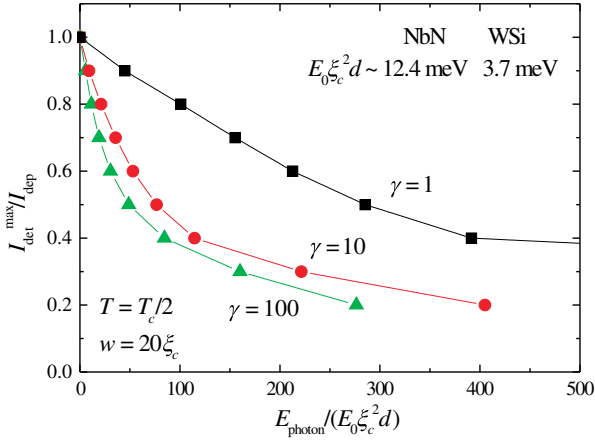
FIG. 10. Dependence of the maximal detection current on the photon's energy at different γ's and at bath temperature $T = T_c/2$ calculated in the 2T hot-spot model. Width of the strip $w = 20\xi_c$ ($\xi_c \simeq 6.4$ nm for NbN with $T_c = 10$ K and $\xi_c \simeq 11$ nm for WSi with $T_c = 3.4$ K). We also present the value of the product $E_0\xi_c^2 d$ for NbN- and WSi-based detectors with the parameters used in Sec. III.

quantitative difference. In the case of a superconductor with a short thermalization time (Fig. 10), one needs a smaller current to detect the single photon—or, at fixed current, the photon—with lesser energy than can be detected by the strip with a large thermalization time (Fig. 5).

In Fig. 11, we present the dependence $I_{det}^{max}(E_{photon})$ for strips of different widths. The most interesting result is that the detection ability of the strip does not depend on its width when $I_{det}^{max}/I_{dep} \gtrsim 0.7$. The effect originates from current crowding around a finite-size spot with a suppressed $|\Delta|$, which leads to instability of the superconducting state at $I \lesssim I_{dep}$ even in the infinitely wide film [2]. Owing to magnetic-field screening by the superconductors, this effect exists only in finite-width strips with
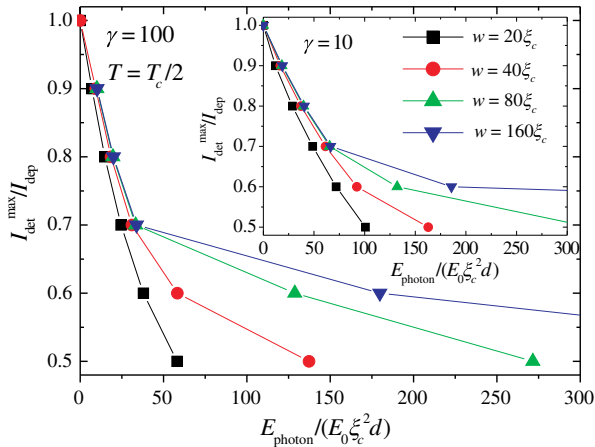
$w \lesssim \Lambda = 2\lambda_L^2/d$, where λ_L is the London penetration depth and screening can be neglected (for a NbN film with the thickness $d = 4$ nm and $\lambda_L \simeq 450$ nm, $\Lambda \simeq 100\mu m \simeq 15800\xi_c$). Analytical calculations in the London model predict that a static normal spot with a radius $R \gg \xi$ destroys the superconducting state in the infinite film at a current $I > 0.5I_{dep}$ [see Eq. (12) in Ref. [2]], while calculations using a stationary Ginzburg-Landau equation give $I \gtrsim 0.7I_{dep}$ (see the inset of Fig. 4 in Ref. [35]). The last result is very close to our finding where, in addition, we take into account the expansion of the hot spot and Joule heating.

As in the case of the hot-belt model, we calculate how the energy of the photon, whose absorption drives the strip to the resistive state, depends on the temperature at a fixed ratio $I/I_{dep}(T)$. From Fig. 12, one can see that this dependence is a nonmonotonic one, as it is in the hot-belt model (compare Figs. 12 and 6).

Finally, we study the effect of the perpendicular magnetic field on I_{det}. The results (see Fig. 13) are similar to the theoretical findings of Ref. [26], where I_{det} is associated with I_{vort} [compare Fig. 13 to Fig. 6(a) in Ref. [26]]. The only difference is that, in the present model, we do not find pinning of the vortices in the strip with $w = 20\xi_c$ at any of the considered T_{init}'s (we find that, in a wider strip, expanding the hot spot can pin the vortices when T_{init} is relatively large). A small variation of I_{det}^{min} in the case of a large T_{init}, we mainly connect with weaker Joule heating as the current decreases, which worsens conditions for the appearance of the growing normal domain. This result correlates with a known effect: that the retrapping current of a superconducting strip has a much weaker field dependence than its critical current (see, for example, the current-voltage characteristics of the NbN strip in Ref. [35]).

FIG. 11. Dependence of the maximal detection current on the photon's energy at $\gamma = 100$ and (inset) $\gamma = 10$ calculated in the 2T hot-spot model for strips with different widths. I_{det}^{max} depends weakly on the width of the strip when $I_{det}^{max}/I_{dep} \gtrsim 0.7$.
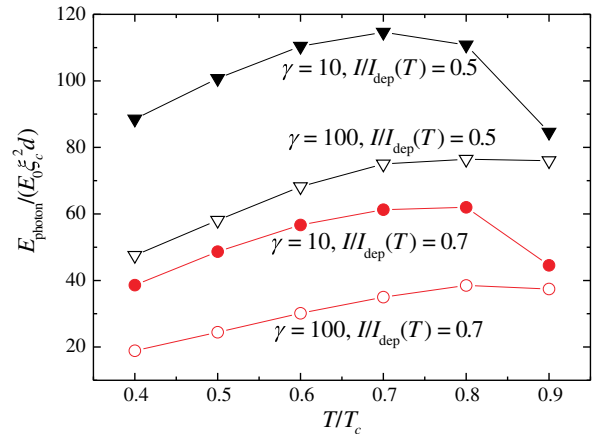
FIG. 12. Dependence of energy of the photon, whose absorption drives the superconducting strip to the resistive state, on temperature at $I/I_{dep}(T) = 0.5$, 0.7 and $\gamma = 10$, 100. Calculations are made in the framework of the 2T hot-spot model.
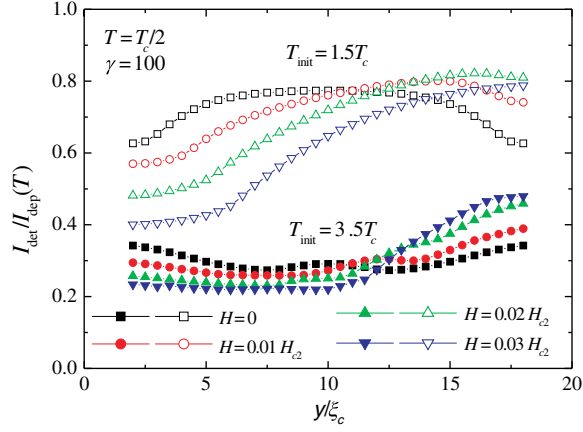
FIG. 13.   Dependence of the detection current on the position of the initial hot spot across the strip at different magnetic fields and two values of T_{init} corresponding to the absorption of photons with different energies ($T_{init} = 1.5T_c \rightarrow E_{photon} \simeq 13.2E_0\xi_c^2 d \simeq 0.05$ eV, $T_{init} = 3.5T_c \rightarrow E_{photon} \simeq 124.5E_0\xi_c^2 d \simeq 0.46$ eV for the parameters of the WSi strip used in Sec. III).

VI. DISCUSSION

A. Electron-phonon down-conversion cascade

The initial stage of an electron-phonon down-conversion cascade on a time scale of $t \lesssim \tau_{|\Delta|}$ is studied in our work using kinetic equations for a spatially uniform system with the volume $V_{init} = \pi\xi^2 d \simeq \pi D\tau_{|\Delta|}d$. In a comparison to previous works [36,37], we take into account e-e inelastic scattering and focus on the question of how the thermalization time, τ_{th}, and the distribution of the photon's energy between the electronic and phonon systems depend on parameters of the superconductor and on time.

By the time $t \simeq \tau_{leak}$ (which is about 1 ps for both the NbN and WSi materials and $E_{photon} \simeq 1$ eV), part of the photon's energy, initially fully absorbed by the electrons, leaks to the phonons, while another fraction stays with the electrons. Subsequent dynamics depends on the relation between τ_{leak} and τ_{th}. When $\tau_{leak} \ll \tau_{th}$ in the time interval $\tau_{leak} < t \lesssim \tau_{th}$, both E_e and E_{ph} vary nonmonotonically in time (with back energy flow from phonons to electrons and vice versa), while, at $t \gg \tau_{th}$, they become time independent. In the case of a short thermalization time, $\tau_{th} \lesssim \tau_{eak}$, such a nonmonotonic dependence is absent and, at $t > \tau_{th} \sim \tau_{leak}$, both E_e and E_{ph} practically do not depend on time and the electrons are thermalized.

We find both analytically and numerically that τ_{leak} is proportional to the energy of the photon and is inversely proportional to the square of the Debye energy. The expression for τ_{leak} [see Eq. (22)] coincides with the expression for time τ_1, introduced in Ref. [37] with the replacement of $3E_1$ by $2\epsilon_0$ [$E_1 \gg \hbar\omega_D$ is determined in Ref. [37] as the energy at which $\tau_{e\text{-}ph}(\epsilon) = \tau_{e\text{-}e}(\epsilon)$]. By

the time $t \simeq \tau_1$ in the model of Ref. [37], practically all of the energy of the photon is transferred to the phonon system. Our calculations show that, by the time $t \simeq \tau_{leak}$, only part of photon's energy goes to the phonons and the size of this part depends on the parameter γ (see Fig. 1).

The thermalization time depends on γ, the strength of the e-e scattering, and the energy of the photon. The larger that $\gamma \sim C_e/C_{ph}|_{T_c}$ is, the larger the part of the photon's energy that finally goes to the electrons and the shorter τ_{th} is. We find that, in the case of a relatively large γ ($\gtrsim 100$) and $E_{photon} \simeq 1$ eV, the thermalization time may be about that of the leakage time—even in the absence of e-e scattering. We also find that, for a typical low temperature, "dirty" superconducting NbN- or WSi-film e-e scattering plays no role in the electron-phonon energy cascade at $t \lesssim \tau_{|\Delta|}$.

In materials with a short τ_{th} ($\simeq\tau_{|\Delta|}$), the electron-phonon down-conversion cascade at $t > \tau_{|\Delta|}$ is connected with a cooling of the electrons and phonons due to the diffusion of hot electrons and the suppression of $|\Delta|$. We study this problem assuming the complete thermalization of electrons at every step of the diffusion process. In this approach, suppression of the superconducting order parameter is described solely by $T_e \neq T$ and instability of the superconducting state occurs before the hot electrons reach both edges of the superconducting strip.

B. Effect of finite escape time and kinetic inductance

In our calculations, we neglect energy flow to the substrate, which is controlled by the escape time of the nonequilibrium phonons, τ_{esc}, in Eq. (2). One also should keep in mind that, in SNSPDs, the current deviates from the superconductor and flow via the shunt when the superconducting strip or meander transits to the resistive state. Both effects obviously should increase I_{det} because a decrease of τ_{esc} enhances a cooling of the electrons, while a decrease of the current weakens Joule heating and worsens the conditions for the appearance and the expansion of the normal domain. An impression about characteristic time scales can be extracted from Fig. 8. The normal domain expands at $t \gtrsim \delta t$ (at such times, voltage grows rapidly) and δt increases with a decreasing I_{det} due to a decrease of Joule dissipation as I^2. Therefore, when $\tau_{esc} \lesssim \delta t$ and the kinetic inductance of the detector L_k is relatively small—thus, $L_k/R_s \lesssim \delta t$ (R_s is averaged over the time-interval $[0, \delta t]$ resistance of the superconductor)—these effects must be taken into account. In Fig. 14, we show the effect of a finite τ_{esc} on the energy-current relation. For a large γ, escape of the nonequilibrium phonons to a substrate has less effect on I_{det} because of the large $C_e/C_{ph}|_{T_c}$ ratio, leading to a rise in the time of the energy transfer from the electronic system to the phonon one and then to the substrate.
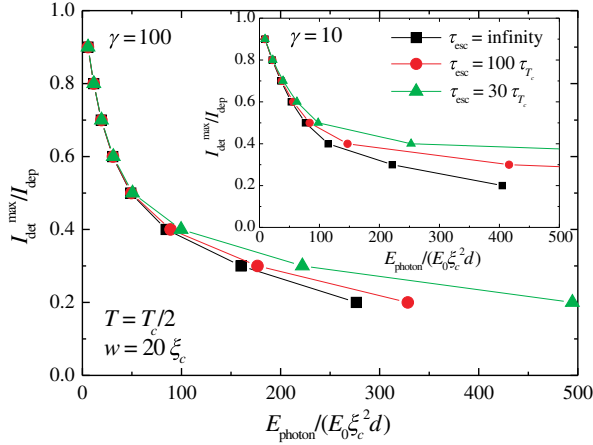
FIG. 14. Dependence of the maximal detection current on the photon's energy at $\gamma = 100$ and different τ_{esc}'s calculated in the 2T hot-spot model. (Inset) Results for $\gamma = 10$.

C. Current-energy relation

Both the hot-belt and 2T hot-spot models predict a nonlinear current-energy relation (see Figs. 5 and 10). The nonlinearity at small energies comes from the nonlinear temperature dependence of the critical (depairing) current and the energy of the electron and phonon systems and, in the case of the hot-spot model, additional nonlinearity comes from the current-crowding effect around the hot spot in a strip with a finite width [38]. Nonlinearity at high energies originates from the existence of a retrapping current, below which the normal domain cannot expand in current-carrying superconductors. Therefore, at high energies, I_{det} should not depend on the photon's energy (at least in modern SNSPDs, where a large voltage signal appears only when a large part of the superconducting strip converts to the normal state) and it should be about that of I_r. The retrapping current goes to zero when $\tau_{esc} \to \infty$ (when the length of the superconductor is much larger than the so-called healing length [39]). That is why, in Figs. 5 and 10, there is no saturation of I_{det} at high energies (in those calculations, $\tau_{esc} = \infty$).

In Ref. [40], a nonlinear current-energy relation was found (see Fig. 12 therein) in a model which resembles our hot-belt model. Kozorezov *et al.* [40] assume that the electrons are thermalized and become uniformly distributed across the strip soon after absorption of the photon. The main difference between our hot-belt model and the approach of Ref. [40] is that we explicitly take into account the heating of the phonons by an absorbed photon and, for simplicity, we neglect the effect of the current on the electronic energy in the superconducting state (the last effect should be important for studying multiphoton detection [41] when relaxation of the hot-spot induced by the first photon at long time periods is determined mainly by electron-phonon inelastic relaxation [40] on the background of a large $|\Delta|$ ($\gg k_B T_e$). In Ref. [40], the part of

the photon's energy which goes to the electronic system is called the energy-deposition factor, and it is considered a fitting parameter which does not depend on E_{photon}. From Eqs. (23)–(25) and (29), it follows that the part of the photon's energy which goes to the electronic system does depend on E_{photon} due to the nonlinear temperature dependencies $\mathcal{E}_e(T)$ and $\mathcal{E}_{ph}(T)$.

An experimentally nonlinear current-energy relation was observed for NbN- and WSi- [26] (in the inset of Fig. 10 from Ref. [26], results for a WSi detector are extracted from the results of Ref. [20]) and MoSi-based [34] detectors. To make a quantitative comparison between theory and experiment, one has to know many material parameters, some of which are known [$N(0)$, T_c, $R_\square$, D] and some of which are not (γ, $\alpha_{e\text{-}e}$, τ_{esc}). The last parameters can be extracted from additional experiments where N_{ion}, ω_D, $\tau_{e\text{-}e}$, and τ_{esc} can be measured. Our calculations of γ for NbN and WSi are based on the N_{ion} found from the molar mass and density of these materials, while the Debye frequency either is taken from the available experimental data (where it varies for different phases of NbN by more than 2 times [15]) or is the result of a reasonable estimation [21]. In the expression for $\alpha_{e\text{-}e}$, we set $a = 1$ [see Eq. (5)], which is not justified by any experiments or rigorous calculations (due to their absence). Taking into account these circumstances and the absence of reliable value for τ_{esc}, we did not make a quantitative comparison with an experiment in our work.

In a theoretical paper [6] by Engel *et al.*, a nearly linear current-energy relation is predicted, and in Ref. [42], such a dependence is observed for a NbN bridge in a large interval of photon's energies (in Ref. [43], current-energy relations for NbN and TaN meanders look like linear ones, but they were found in a narrow energy interval and could be fitted by nonlinear functions with only one fitting parameter; see Ref. [38]). An experiment shows [44] that, for a WSi bridge, the current-energy relation is also nearly linear, with a small deviation from linear behavior at low energies. The reason for the discrepancy between experimental results found in the meander and the bridge geometry is not clear at the moment. For example, it could be connected to the nonuniform current distribution which appears naturally in the bridge whose length is comparable to its width. In such a geometry, the current density is maximal near the edges of the bridge, which definitely should affect the position-dependent detection current and may influence the current-energy dependence quantitatively.

D. Temperature-dependent cutoff wavelength

It has been found in many experiments that the detection efficiency of SNSPDs at fixed current drops very fast at wavelengths larger than some critical value (referred to as the cutoff wavelength, λ_c, or the red-boundary wavelength [16,43]). Systematic measurements of $\lambda_c(T)$ in Ref. [45] reveal that λ_c decreases with an increase in the temperature (in the considered temperature interval $0.05 T_c$–$0.6 T_c$)

when one keeps the $I/I_{dep}(T)$ ratio constant. It is in contrast to the naive expectation that, as $T \to T_c$ and $|\Delta|$ decreases, one needs a lower energy photon (having a longer wavelength) to destroy superconductivity.

We calculate the cutoff photon's energy at different temperatures and a fixed $I/I_{dep}(T)$ ratio in hot-belt (see Fig. 6) and 2T hot-spot (see Fig. 12) models. Both models predict an increase of cutoff energy (a decrease of λ_c) with a temperature increase when $T \lesssim T_1$ $[T_1 = 0.6T_c–0.8T_c$, depending on the model, the $I/I_{dep}(T)$ ratio, and the parameter γ]. In both models, the effect mainly comes from the nonlinear temperature dependence of the electronic and phonon energies (see the discussion around Fig. 7).

E. Photon detection at temperatures near T_c

As $T \to T_c$, both models predict a decrease of cutoff energy (an increase of λ_c) in the temperature interval $0.6T_c–0.8T_c \lesssim T < T_c$ when one does not take into account expansion of the normal domain. When $I < I_r(T)$, the normal domain cannot expand in the superconducting strip and SNSPDs should lose their ability to detect single photons. Because $I_r(T) = I_c(T)$ $[I_c(T)$ is the critical current of the real meander or strip], at some temperature T^* close to T_c, the detector cannot detect single photons when $T \gtrsim T^*$. Actually, it can stop detecting single photons even at lower temperatures. Indeed, the retrapping current is determined from the balance between Joule heating and heat removal to the substrate. For a relatively short normal domain (with a length shorter than the thermal healing length η [39]), additional heat removal comes from the diffusion of hot electrons from the hot spot, which increases I_r. From Eqs. (30) and (31), it follows that the healing length at $T_e \simeq T_c$ and $|T_e - T_c| \ll T_c$ is $\eta = [2\pi^2 D\tau_0/1440\zeta(5)]^{1/2}[(1+\alpha)/\alpha]^{1/2}$, where $\alpha = \pi^4\tau_0/[450\zeta(5)\gamma\tau_{esc}]$. With the parameters used for NbN, $\tau_0 = 270$ ps and $\tau_{esc} \simeq 20$ ps, we find that $\alpha \simeq 0.3$ and $\eta \simeq 29$ nm $\simeq 4.5\xi_c$, which is larger or comparable to the radius of a hot spot when it drives the current-carrying superconducting strip to the resistive state (the radius of such a hot spot can be extracted for different E_{photon}'s from Fig. 8; I_{det} is minimal for a hot spot which touches the edge of the strip [5,26]).

F. Magnetic field as a probe for detection mechanism

Current-energy relation and temperature dependence of cutoff photon's energy following from hot-belt and 2T hot-spot models are qualitatively the same. To distinguish which model is related to the experiment, one needs to make a quantitative comparison, but it is difficult to do so due to the lack of many material parameters. However, the response of the detector to a magnetic field is *qualitatively* different in hot-belt and hot-spot models. In the hot-belt model (and in any model which assumes a uniform, across

the strip distribution of nonequilibrium electrons), the applied magnetic field increases detection efficiency at *any* current [26] (or does not change it if DE reaches a plateau at high current). In the hot-spot model, due to a position-dependent I_{det}, a weak magnetic field may decrease DE in a finite interval of currents [26]. Therefore, the magnetic field plays the role of a *qualitative* probe for the detection mechanism.

G. Single-photon detection by a micron-wide strip

In the hot-spot model, detection of a relatively high-energy photon by a wide thin strip (with a width of up to several microns) does not depend on its width if it can carry a superconducting current larger than $0.7I_{dep}$ (see Fig. 11 and the accompanying text). It brings a qualitative difference with a hot-belt model where the detection ability depends strongly on the width of the strip at any current. Experimental observation of this effect could open the way for an alternative design of SNSPDs in the form of a wide bridge, which has a much smaller kinetic inductance than present meander-type detectors and, hence, much shorter voltage pulses. Nowadays, detectors based on NbN or TaN have a critical current up to $0.6I_{dep}$ [43], which is not large enough (see Fig. 11) for an implementation of this idea.

H. Single-photon detection by a high-T_c superconducting strip

Let us discuss perspectives of high-T_c materials to be used as active elements in SNSPDs. For simplicity, we use the normal-spot (NS) model and neglect the current-crowding effect and the position dependence of the detection current. In this oversimplified model, the radius of a normal hot spot can be found using Eq. (23) with the replacement $w^2 \to \pi R^2$, $T_e = T_c$ and assuming a bath temperature $T \ll T_c$ [in this case, $\mathcal{E}_s(T) \simeq 0.4$]:

$$R_{NS} = \sqrt{\frac{E_{photon}}{4\pi dN(0)(k_B T_c)^2}}\sqrt{\frac{1}{\pi^2/12 + \pi^4/(\gamma 15) + 0.4}}. \tag{38}$$

In this model, the detection current linearly depends on the radius of the normal spot and does not depend on its position,

$$\frac{I_{det}}{I_{dep}} = \left(1 - \frac{2R_{NS}}{w}\right), \tag{39}$$

which is a consequence of neglecting the current-crowding effect and the assumption that the photon absorbed near the edge of the strip creates a normal spot of the same shape (a circle) as the photon absorbed in the center of the strip.

This normal-spot model gives an order-of-magnitude-correct estimation when (i) the current is smaller than

$0.5I_{dep}$ (but larger than the retrapping current), and (ii) $R_{NS} \gtrsim w/4$ and the effect of current crowding is relatively small [see Fig. 4 in Ref. [35] for a comparison of Eq. (39) to a numerical result where this effect is taken into account for a normal spot located in the center of the strip]. Indeed, for parameters of the NbN-based detector from Ref. [26], which demonstrated an intrinsic detection efficiency (IDE) of about unity at $I/I_{dep} \simeq 0.5$ for a photon with the wavelength $\lambda = 1000$ nm (see Fig. 2 in Ref. [26]) and $\gamma = 9$, one finds $R_{NS} \simeq 26$ nm from Eq. (38). With the help of Eq. (39) and with $w = 100$ nm, we get $I_{det}/I_{dep} \simeq 0.5$, which is close to the experimental value. However, in a superconductor with $T_c = 100$ K and the same other material parameters, such a photon creates a hot spot with a radius 10 times smaller ($R_{NS} \simeq 2.6$ nm), and one needs a strip with a width $w \simeq 10$ nm to detect this photon with IDE $\simeq 1$ at $I = 0.5I_{dep}$. The actual width should be even smaller because parameter γ is approximately equal to $1/T_c^2$ [see Eq. (7)], which additionally decreases the radius of the normal spot.

The situation differs at currents larger than about $0.7I_{dep}$, where the energy of the photon weakly depends on the width of the strip (see Fig. 11). For example, for a NbN detector in Ref. [26] and a photon with $\lambda = 1000$ nm, $E_{photon}/E_0\xi_c^2 d \simeq 100$, while, for a superconductor with $T_c = 100$ K and the same other parameters, $E_{photon}/E_0\xi_c^2 d \simeq 10$, which means that one needs a current of about $0.9I_{dep}$ to have an IDE $\simeq 1$, but with no limit for the width (while it is smaller than the Pearl length).

The above arguments show that the use of a high-T_c material in SNSPDs necessitates a much narrower strip than a low-T_c material requires or that a strip must be of very high quality to have a critical current of about 90% of the depairing current to detect an optical or near-infrared photon with an intrinsic detection efficiency of about unity.

VII. CONCLUSION

Our main conclusions are as follows:
(1) After absorption of the near-infrared or optical photon by a dirty superconducting strip, the thermalization time of both electrons and phonons can be of about the time variation of magnitude of superconducting order parameter $\tau_{|\Delta|}$ when the radius of the hot spot does not exceed the superconducting coherence length. Such a situation can be realized in superconductors with a relatively small diffusion coefficient ($D \simeq 0.5$ cm^2/s) and a large $C_e/C_{ph}|_{T_c}$ ratio ($\gg 1$).
(2) At times $t > \tau_{|\Delta|}$, the hot electrons are cooled due to their diffusion, energy exchange with phonons, and suppression of $|\Delta|$ inside the expanding hot spot. The larger the energy of the photon, the larger the size of the hot spot where the local temperature $T_e \gtrsim T_c$ and the superconducting state becomes unstable at smaller currents.
(3) Instability is connected with the nucleation and motion of the vortices before the hot spot expands over the whole width of the strip. However, vortex motion leads to the appearance of a growing normal domain only at currents larger than the so-called detection current, whose value depends on the energy of the photon, the place where the photon is absorbed and the magnetic field. The detection current cannot be smaller than the retrapping current of the strip.
(4) In superconductors with a small $C_e/C_{ph}|_{T_c}$ ratio ($\ll 1$), detection of a near-infrared or optical photon is possible only at a current close to the depairing current in the strip with a width $w \geq 20\xi_c$ because only a small fraction of the photon's energy goes to the electrons. We may make the same conclusion for superconductors with a large diffusion coefficient because, in this case, the size of the hot spot is pretty large by the time that the electrons are thermalized (hot electrons may form the hot belt across the strip), which leads to locally smaller heating and a weaker influence on the superconducting properties.

Calculations made for WSi with material parameters available from the literature allow us to conclude that the hot-belt model should be irrelevant for detectors made from this material and a strip with $w = 150$ nm because $\tau_{D,w} \simeq w^2/16D \simeq 28$ ps, which is much larger than $\tau_{th} \simeq 0.36$ ps (see Sec. III). We can make the same conclusion for NbN materials despite the absence of complete thermalization of the electrons at the initial stage of hot-spot formation. This conclusion is mainly based on the experimental results of Ref. [26], which support the hot-spot model with a strongly suppressed $|\Delta|$ inside the hot spot. Only for high-energy photons—when $I_{det} \ll I_{dep}$ and the size of the expanding hot spot, which drives the superconductor to the resistive state, is comparable to the width of the strip—may one expect the hot-belt model to give reasonable results. The hot-belt model can be also useful for the study of two-photon detection [40,41], where there is a time delay between the absorption of two photons and the hot region can expand over the whole width of the superconducting strip.

[1] A. Semenov, A. Engel, H.-W. Hubers, K. Il'in, and M. Siegel, Spectral cut-off in the efficiency of the resistive state formation caused by absorption of a single-photon in

current-carrying superconducting nano-strips, Eur. Phys. J. B **47**, 495 (2005).

[2] A. N. Zotova and D. Y. Vodolazov, Photon detection by current-carrying superconducting film: A time-dependent Ginzburg-Landau approach, Phys. Rev. B **85**, 024509 (2012).

[3] L. N. Bulaevskii, M. J. Graf, and V. G. Kogan, Vortex-assisted photon counts and their magnetic field dependence in single-photon superconducting detectors, Phys. Rev. B **85**, 014505 (2012).

[4] A. Eftekharian, H. Atikian, and A. H. Majedi, Plasmonic superconducting nanowire single photon detector, Opt. Express **21**, 3043 (2013).

[5] A. N. Zotova and D. Y. Vodolazov, Intrinsic detection efficiency of superconducting nanowire single photon detector in the modified hot spot model, Supercond. Sci. Technol. **27**, 125001 (2014).

[6] A. Engel, J. Lonsky, X. Zhang, and A. Schilling, Detection mechanism in SNSPD: Numerical results of a conceptually simple, yet powerful detection model, IEEE Trans. Appl. Supercond. **25**, 2200407 (2015).

[7] A. Engel, J. J. Renema, K. Il'in, and A. Semenov, Detection mechanism of superconducting nanowire single-photon detectors, Supercond. Sci. Technol. **28**, 114003 (2015).

[8] A. Rothwarf and B. N. Taylor, Measurement of Recombination Lifetimes in Superconductors, Phys. Rev. Lett. **19**, 27 (1967).

[9] G. M. Eliashberg, Inelastic electron collisions and nonequilibrium stationary states in superconductors, Zh. Eksp. Teor. Fiz. **61**, 1254 (1971).

[10] A. M. Gulyan and G. F. Zharkov, Electron and phonon kinetics in a nonequilibrium Josephson junction, Sov. Phys. JETP **62**, 89 (1985).

[11] S. B. Kaplan, C. C. Chi, D. N. Langenberg, J. J. Chang, S. Jafarey, and D. J. Scalapino, Quasiparticle and phonon lifetimes in superconductors, Phys. Rev. B **14**, 4854 (1976).

[12] J. J. Chang and D. J. Scalapino, Kinetic-equation approach to nonequilibrium superconductivity, Phys. Rev. B **15**, 2651 (1977).

[13] J. Rammer and H. Smith, Field-theoretical methods in transport theory, Rev. Mod. Phys. **58**, 323 (1986).

[14] B. L. Altshuler and A.G Aronov, in *Electron-Electron Interaction in Disorder Systems*, edited by A. L. Efros and M. Pollok (North-Holland, Amsterdam, 1985).

[15] Y. Zou, X. Wang, T. Chen, X. Li, X. Qi, D. Welch, P. Zhu, B. Liu, T. Cui, and B. Li, Hexagonal-structured ϵ-NbN: Ultra-incompressibility, high shear rigidity, and a possible hard superconducting material, Sci. Rep. **5**, 10811 (2015).

[16] A. Engel, A. Aeschbacher, K. Inderbitzin, A. Schilling, K. Il'in, M. Hofherr, M. Siegel, A. Semenov, and H.-W. Hubers, Tantalum nitride superconducting single-photon detectors with low cut-off energy, Appl. Phys. Lett. **100**, 062601 (2012).

[17] A. Schmid and G. Schon, Linearized kinetic equations and relaxation processes of a superconductor near T_c, J. Low Temp. Phys. **20**, 207 (1975).

[18] A. D. Semenov (private communication); A. D. Semenov, R. S. Nebosis, Yu. P. Gousev, M. A. Heusinger, and K. F. Renk, Analysis of the nonequilibrium photoresponse of superconducting films to pulsed radiation by use of a two-temperature model, Phys. Rev. B **52**, 581 (1995).

[19] URL: https://en.wikipedia.org/wiki/Niobium_nitride.

[20] B. Baek, A. E. Lita, V. Verma, and S. W. Nam, Superconducting a- W_xSi_{1-x} nanowire single-photon detector with saturated internal quantum efficiency from visible to 1850 nm, Appl. Phys. Lett. **98**, 251105 (2011).

[21] M. Sidorova, A. Semenov, A. Korneev, G. Chulkova, Yu. Korneeva, M. Mikhailov, A. Devizenko, A. Kozorezov, and G. Goltsman, Electron-phonon relaxation time in ultrathin tungsten silicon film, arXiv:1607.07321.

[22] X. Zhang, A. Engel, Q. Wang, A. Schilling, A. Semenov, M. Sidorova, H.-W. Hübers, I. Charaev, K. Ilin, and M. Siegel, Characteristics of superconducting tungsten silicide W_xSi_{1-x} for single photon detection, Phys. Rev. B **94**, 174509 (2016).

[23] M. Tinkham, J. U. Free, C. N. Lau, and N. Markovic, Hysteretic I–V curves of superconducting nanowires, Phys. Rev. B **68**, 134515 (2003).

[24] D. Hazra, L. M. A. Pascal, H. Courtois, and A. K. Gupta, Hysteresis in superconducting short weak links and μ-SQUIDs, Phys. Rev. B **82**, 184530 (2010).

[25] F. Marsili, V. B. Verma, J. A. Stern, S. Harrington, A. E. Lita, T. Gerrits, I. Vayshenker, B. Baek, M. D. Shaw, R. P. Mirin, and S. W. Nam, Detecting single infrared photons with 93% system efficiency, Nat. Photonics **7**, 210 (2013).

[26] D. Yu. Vodolazov, Yu. P. Korneeva, A. V. Semenov, A. A. Korneev, and G. N. Goltsman, Vortex-assisted mechanism of photon counting in superconducting nanowire single photon detector revealed by external magnetic field, Phys. Rev. B **92**, 104503 (2015).

[27] K. K. Nagaev, Influence of electron-electron scattering on shot noise in diffusive contacts, Phys. Rev. B **52**, 4740 (1995).

[28] D. Yu. Vodolazov and F. M. Peeters, Temporary cooling of quasiparticles and delay in voltage response of superconducting bridges after abruptly switching on the supercritical current, Phys. Rev. B **90**, 094504 (2014).

[29] M. I. Kaganov, I. M. Lifshitz, and L. V. Talanov, Zh. Eksp. Teor. Fiz. **31**, 232 (1956).

[30] N. Perrin and C. Vanneste, Response of superconducting films to a periodic optical irradiation, Phys. Rev. B **28**, 5150 (1983).

[31] R. J. Watts-Tobin, Y. Krähenbühl, and L. Kramer, Nonequilibrium theory of dirty, current-carrying superconductors: Phase-slip oscillators in narrow filaments near T_c, J. Low Temp. Phys. **42**, 459 (1981).

[32] A. Schmid, in *Nonequilibrium Superconductivity, Phonons, and Kapitza Boundaries*, edited by K. E. Gray (Plenum Press, New York, 1981), p. 423.

[33] J. J. Renema, Q. Wang, R. Gaudio, I. Komen, K. op 't Hoog, D. Sahin, A. Schilling, M. P. van Exter, A. Fiore, A. Engel, and J. A. de Dood, Position-dependent local detection efficiency in nanowire superconducting single-photon detector, Nano Lett. **15**, 4541 (2015).

[34] M. Caloz, B. Korzh, N. Timoney, M. Weiss, S. Gariglio, R. J. Warburton, Ch. Schonenberger, J. Renema, H. Zbinden, and F. Bussieres, Optically probing the detection mechanism in a molybdenum silicide superconducting

nanowire single-photon detector, Appl. Phys. Lett. **110,** 083106 (2017).

[35] D. Yu. Vodolazov, K. Ilin, M. Merker, and M. Siegel, Defect-controlled vortex generation in current-carrying narrow superconducting strips, Supercond. Sci. Technol. **29,** 025002 (2016).

[36] Yu. N. Ovchinnikov and V. Z. Kresin, Nonstationary state of superconductors: Application to nonequilibrium tunnelling detectors, Phys. Rev. B **58,** 12416 (1998).

[37] A. G. Kozorezov, A. F. Volkov, J. K. Wigmore, A. Peacock, A. Poelaert, and R. den Hartog, Quasiparticle-phonon downconversion in nonequilibrium superconductors, Phys. Rev. B **61,** 11807 (2000).

[38] D. Yu. Vodolazov, Current dependence of the red boundary of superconducting single-photon detectors in the modified hot-spot model, Phys. Rev. B **90,** 054515 (2014).

[39] W. J. Skocpol, M. R. Beasley, and M. Tinkham, Self-heating hotspots in superconducting thin-film microbridges, J. Appl. Phys. **45,** 4054 (1974).

[40] A. G. Kozorezov, C. Lambert, F. Marsili, M. J. Stevens, V. B. Verma, J. A. Stern, R. Horansky, S. Dyer, S. Duff, D. P. Pappas, A. Lita, M. D. Shaw, R. P. Mirin, and S. W. Nam, Quasiparticle recombination in hotspots in superconducting current-carrying nanowires, Phys. Rev. B **92,** 064504 (2015).

[41] F. Marsili, M. J. Stevens, A. Kozorezov, V. B. Verma, Colin Lambert, J. A. Stern, R. D. Horansky, S. Dyer, S. Duff, D. P. Pappas, A. E. Lita, M. D. Shaw, R. P. Mirin, and S. W. Nam, Hotspot relaxation dynamics in a current-carrying super-conductor, Phys. Rev. B **93,** 094518 (2016).

[42] J. J. Renema, R. Gaudio, Q. Wang, Z. Zhou, A. Gaggero, F. Mattioli, R. Leoni, D. Sahin, M. J. A. de Dood, A. Fiore, and M. P. van Exter, Experimental Test of Theories of the Detection Mechanism in a Nanowire Superconducting Single Photon Detector, Phys. Rev. Lett. **112,** 117604 (2014).

[43] R. Lusche, A. Semenov, K. Ilin, M. Siegel, Y. Korneeva, A. Trifonov, A. Korneev, G. Goltsman, D. Vodolazov, and H.-W. Hubers, Effect of the wire width on the intrinsic detection efficiency of superconducting nanowire single-photon detectors, J. Appl. Phys. **116,** 043906 (2014).

[44] R. Gaudio, Z. Zhou, A. Fiore, J. J. Renema, M. P. van Exter, M. J. A. de Dood, V. B. Verma, A. E. Lita, J. Shainline, M. J. Stevens, R. P. Mirin, and S. W. Nam, Experimental inves-tigation of the detection mechanism in WSi nanowire superconducting single photon detectors, Appl. Phys. Lett. **109,** 031101 (2016).

[45] A. Engel, K. Inderbitzin, A. Schilling, R. Lusche, A. Semenov, H.-W. Hubers, D. Henrich, M. Hofherr, K. Il'in, and M. Siegel, Temperature-dependence of detection efficiency in NbN and TaN SNSPD, IEEE Trans. Appl. Supercond. **23,** 2300505 (2013).